Ministry of Higher Education and Scientific Research
University of Baghdad
Institute of Laser for Postgraduate Studies

Enhancement of Quantum Repeater Performance Using Non-Identical Memories with Cut-off Notion

A Thesis Submitted to the Institute of Laser for Postgraduate Studies, University of Baghdad in Partial Fulfillment of the Requirements for the Degree of Master of Science in Laser / Electronic and Communication Engineering

By

Marwa Asaad Khalid

B.Sc. Electronics and Communications Engineering – 2009

Supervisor

Lecturer: Dr. Jawad A. Hasan

2019 AD 1441 AH


يَرْفَعِ اللَّهُ الَّذِينَ آمَنُوا مِنْكُمْ
وَالَّذِينَ أُوتُوا الْعِلْمَ دَرَجَاتٍ

Dedication

To express my gratitude to those who supported and encouraged me, I dedicate this dissertation

To

The Big Hearts ... My mother and my father

My beloved husband 'Mohammed''

My loving son ''Rayan''

My Brothers and My

Friends who encourage and

Support me.

Marwa

Acknowledgment

I would like to express my deep gratitude and appreciation to my supervisor, **Dr.Jawad A. Hasan** for his advice, guidance, helpful suggestion, encouragement and his expensive time that he gave during this work.

Great appreciation is to **Adnan N. Kadhim**, for his continuous support and help during my research work.

I would also like to thank my distinguished professors for their great help and support.

Finally, special thanks to students of the Institute of Laser for Postgraduate for their help and encouragement.

Abstract

The aim of any communication system is the transmission of the information over long distances with less error. Transition of the information directly for long distance between two points (Alice and Bob) connected by an optical fiber is difficult attributed to the exponential decay of light transmission efficiency with the length of the optical fiber. Hence, to overcome this issue, the distance must be divided into small distances by introducing intermediate station between them; this station is known as a quantum repeater.

One of the schemes of the quantum repeater used the concept of cut-off with identical quantum memories in the quantum repeater, that is the quantum repeater sends one entangled photon with the first quantum memory to Alice for many times until the detection, then the quantum repeater sends one entangled photon with the second quantum memory to Bob for specific number of trails (cut-off). If Bob makes until detection before the cut-off, Bell state measurement is applied and if not the round will abort and start over again. This protocol reduces the decoherence of the quantum memories with time, in order to implement this protocol the probability of Bob must be larger than or equal to the probability of Alice.

In the original idea the probabilities of Alice and Bob are equal because identical quantum memories are used and the equality of probabilities remains if any type of quantum memory is used. To make the probability of Bob greater than the probability of Alice, this scheme proposed different quantum memories in the quantum repeater to get best number of cut-off and maximize the secret key rate. The secret key rate obtained is $1.04372442*10^{-3}$, $1.47772778*10^{-5}$ for the cut off number 50 and $1.15652165*10^{-3}$, $2.08223733*10^{-5}$ for cut off number 100 for distance 100km and 200km respectively.

Contents

List of Abbreviations

BSM	Bell state measurement
CNOT	Controlled NOT gate
DFG	Difference frequency generation
EPR	Einstein, Podolsky, Rosen,
H gate	Hadamard gate
NV center	Nitrogen-vacancy center
POVM	Positive operator valued measure
qubit	Quantum bit
QBER	Quantum bit error rate
QKD	Quantum key distribution
QM	Quantum memory
QR	Quantum repeater
RZ	Radio frequency
SFG	Sum frequency generation
Tr	Trace operator

List of symbols

L_{att}	attenuation length
F_{prep}	dephasing parameter of preparation fidelity
α	depolarising parameter
F_{gm}	depolarizing parameter of the noise introduced by imperfect gates and measurements
$\|E(x)\|$	energy magnitude
ex, eY , ez.	error rates in the x, Y and z bases
Fc	frequency conversion
$BB84$	$BB84$ protocol
$\sigma_x, \sigma_y, \sigma_z$	Pauli matrices in x, y, z
t_{prep}	Preparation time for the emission of an entangled photon.
p_d	probability of a dark count
P_c	probability of coupling the quantum memory with fiber
n*	specific number of trails
c	speed of light in vacuum
R_{TGW}	Takeoka-Guha-Wilde rate
$h(e)$	the binary entropy function
Lb	the distance from the quantum repeater to Bob
R	The secret key rate
P_{det}	the probability of detect the photons
P_{em}	the probability of generating photon from quantum memory into the optical fiber
n_{ri}	the refractive index of the fiber
δ	transmissivity of optical fiber
$\|\varphi\rangle$	vector space

List of Figures

List of Tables

Chapter One
Introduction and Basic Concepts

1.1 Introduction

Quantum communication is the transmission and sharing of quantum information between parties of a quantum network. It allows the achievement of communication tasks inaccessible to their classical counterparts [1– 4]. The most well- known example is the distribution of the secret keys [5- 8]. Actually, both classical and quantum data transmitted for long distances over optical fibers decays exponentially with the distance. In order to overcome this problem, in the classical communication the stations are pulling in the way of classical data to amplify them and increasing the transmission rate, but in quantum communication, the amplification of a quantum state is restricted due to the no-cloning theorem [9]. Therefore, this obstacle can be overcome by introducing a quantum repeater.

Quantum repeaters (QRs), extend the transmission distance without amplifying the signals and transmit data at a rate (in bits per mode per channel use) surpassing the capacity of the quantum channel [10-12]. The essential thought of a quantum repeater was proposed in [11] which based on divide the overall channel that separates Alice and Bob into smaller segments that are linked to the quantum repeater. The entanglement is generated over those segments, and then the entanglement swapping operation is performed on each quantum repeater in a nested way to produce a long-distance entanglement. The noise problem can be solved by using entanglement distillation [13- 15].

One of the realistic quantum repeater configurations is a single sequential quantum repeater located in middle of the distance that separates Alice and Bob [16] with a specific amount of trials which called the cut-off (n*). This

approach reduces the decoherence of the quantum state that is stored in quantum memories.

The condition of having a cut-off is that the probability of detection a photon in Bob side must be greater or equal to the probability of detection a photon in Alice side. So the increment in Bob's probability leads to increase in the secret key rate that is exchanged between Alice and Bob, so the use of different quantum memories in quantum repeater is proposed.

1.2 Aim of the Work

In this work a scheme of a quantum repeater based on a non-identical quantum memories assisted by a cut-off protocol is suggested. The quantum repeater memories are Nitrogen Vacancy center and trapped ion quantum memories. The work aims to study the effect of the cut-off on the performance of the quantum repeater and compare the proposed scheme with the original scheme.

1.3 Fundamentals of Quantum Mechanics

1.3.1 Quantum bits

As the bit is the unit of classical information, the quantum bit (qubit) is the unit of the quantum information. The qubit $|\varphi\rangle$ is represented mathematically as [17]:

$$|\varphi\rangle = \alpha|0\rangle + \beta|1\rangle \qquad (1.1)$$

Where $|0\rangle$ and $|1\rangle$ form an orthonormal basis in the state space, α and β represent the probability amplitudes associated with the basis states. The qubit state vector must have unit norm, $|\alpha|^2 + |\beta|^2 = 1$.

The computational basis (Z basis) is given by [17]:

$$|0\rangle = \begin{bmatrix}1\\0\end{bmatrix}, |1\rangle = \begin{bmatrix}0\\1\end{bmatrix} \qquad (1.2)$$

And the diagonal basis (X basis) is defined by [17]:

$$|+\rangle = \frac{1}{\sqrt{2}}(|0\rangle + |1\rangle)\,, |-\rangle = \frac{1}{\sqrt{2}}(|0\rangle - |1\rangle) \quad (1.3)$$

Similarly, the state $|\varphi\rangle$ of the two qubits will be any normalized superposition of the four orthogonal bases states as show [17]:

$$|\varphi\rangle = \alpha_{00}|00\rangle + \alpha_{01}|01\rangle + \alpha_{10}|10\rangle + \alpha_{11}|11\rangle \quad (1.4)$$

In which, the complex amplitudes are confined by normalized condition [17]:

$$|\alpha_{00}|^2 + |\alpha_{01}|^2 + |\alpha_{10}|^2 + |\alpha_{11}|^2 = 1 \quad (1.5)$$

So, for n qubits the states will be [19]:

$$|\varphi\rangle = \sum_{0\leq x< 2^n} \alpha_x\, |x\rangle_n \quad (1.6)$$

$$\sum_{0\leq x< 2^n} |\alpha_x|^2 = 1 \quad (1.7)$$

The Pauli matrices which are shown below are helpful in the quantum computing investigation and quantum information [18]

$$\sigma_0 \equiv I \equiv \begin{bmatrix} 1 & 0 \\ 0 & 1 \end{bmatrix} \qquad \sigma_1 \equiv \sigma_x \equiv \begin{bmatrix} 0 & 1 \\ 1 & 0 \end{bmatrix} \quad (1.8)$$

$$\sigma_2 \equiv \sigma_y \equiv \begin{bmatrix} 0 & -i \\ i & 0 \end{bmatrix} \qquad \sigma_3 \equiv \sigma_z \equiv \begin{bmatrix} 1 & 0 \\ 0 & -1 \end{bmatrix}$$

1.3.2 State space and operators

Any system can be identified by its state vector; the state vector is a unit vector in the state space of the system or in Hilbert space which is indicated by (H). The simplest example of this system in quantum mechanical is the qubit, which has a two-dimensional state space. The $|0\rangle$ and $|1\rangle$ are the orthonormal basis for this state space. Then an arbitrary state vector in the state space can be written as equation (1.1). In the closed system, evolution operator is used to transform the state vector into another

state vector in the same state space. The unitary operator (U) must satisfy the condition $U^{\dagger}U= I$, and the Hermitian operator satisfies the property $U^{\dagger} = U$, these two properties must be satisfied and must be positive semi-definite in order to ensure eigenvalues are real and positive. Mathematically, the operators are described by a matrix [18].

1.3.3 Inner and Tenser product

When two vectors $|v\rangle$ and $|w\rangle$ have an inner product function between them, the output is a complex number. The quantum mechanical abbreviated notation for this function is $\langle v \mid w\rangle$ where $|v\rangle$ and $|w\rangle$ are vectors in the inner product space. The inner product is given by [18]:

$$\big((y_1,\ldots,y_n),(z_1,\ldots,z_n)\big) \equiv \sum_i y_i^* z_z \;=\; [y_{1\ldots.}^* y_n^*] \begin{bmatrix} z_1 \\ . \\ . \\ z_n \end{bmatrix} \qquad (1.9)$$

The second function is the tensor product which is used to produce larger vector spaces as shown (1.10). The standard quantum mechanical notation for the tensor product is $|v\rangle|w\rangle$, $|v, w\rangle$ or $|v\ w\rangle$ for the tensor product $|v\rangle \otimes |w\rangle$. For example, the tensor product of the vectors (1, 2) and (5, 2) will produce the vector

$$\begin{bmatrix}1\\2\end{bmatrix} \otimes \begin{bmatrix}5\\2\end{bmatrix} = \begin{bmatrix}5\\2\\10\\4\end{bmatrix} \qquad (1.10)$$

1.3.4 Measurements

The measurement is introduced by a group of Kraus operators, symbolized by $\{M_i\}$. When the system is in the state $|\varphi\rangle$ before the measurement, then a measuring probability of the i-th result is [17]:

$$P_i = \langle\varphi|M_i^\dagger M_i|\varphi\rangle \quad (1.11)$$

After the measurement, the result (i) is known to an observer, so the original state will be [17]:

$$|\varphi\rangle = \frac{M_i|\varphi\rangle}{\langle\varphi|M_i^\dagger M_i|\varphi\rangle} \quad (1.12)$$

The set of measurement operators must satisfy the completeness relation, which ensures that the probabilities p_i sum to 1. The completeness relation is given by [17]:

$$\sum_i M_i^\dagger M_i = I \quad (1.13)$$

The simplest measurement operators can be defined as Projective measurements or von Neumann measurements which is denoted by P

Projectors properties are [17]:

* self-adjoint operators satisfying the condition $P_m^\dagger = P_m$.

* Moreover $P_m P_m = P_m$

* Projective measurement elements are orthogonal $P_m P_n = \delta_{(m-n)} P_m$, projecting quantum states into orthogonal subspaces.

At most the set $\{M_i\}$ can contain d elements, where d is the dimension of the Hilbert space being measured. Measurement operators can be generalized the by defining a set $\{F_m\}$, where $F_m = M^\dagger_m M_m$. This set is known as positive value-operator measure (POVM). POVM elements are not necessarily orthogonal, so that is implying that there can be more elements in the set $\{F_m\}$ than the size of the original Hilbert space [17].

1.3.5 Density matrix

Density matrix or density operator can be represented by taking the outer product of the ket and bra vectors, where ket is a quantum state and bra is the transposed complex conjugate of ket [18],

$$\rho = |\varphi\rangle\langle\varphi| \quad (1.14)$$

The Density matrix properties are:

- (Trace condition) - has trace equal to one.
- (Positivity condition) - is a positive operator.

1.3.6 Trace operator

The trace of a density matrix can be defined as the sum of diagonal entries of density matrix. For a square matrix A with (n × n) dimension, the trace operator (Tr) for this matrix is given by [19]:

$$Tr\,(\mathrm{A}) = a_{11} + a_{22} + \ldots + a_{nn} = \sum_{i=1}^{n} a_{ii} \quad (1.15)$$

a_{ii} are the elements of the main diagonal. Also by the trace of the matrix A, the sum of the eigenvalues of its matrix can be found [19].

$$Tr\,(\mathrm{A}) = \sum_{i=1}^{n} \lambda_i \quad (1.16)$$

Where, the eigenvalue is the factor by which the eigenvector changes if it is multiplied by the matrix A, for each eigenvector. When the eigenvectors of the square matrix A multiplied by the matrix A, the direction of them will remain the same to the original vector. So, the eigenvectors remain proportional to the original vector.

For square matrix *A*, the eigenvector of *A* is the non-zero vector **v**, if there is a scalar λ for which [19]

$$A\mathbf{v} = \lambda\,\mathbf{v} \quad (1.17)$$

Where λ is the eigenvalue of *A* corresponding to the eigenvector **v**. By using the eigenvalues, the spectral decomposition of density matrix ρ can be shown as [19]:

$$\rho = \sum_i \lambda_i |\varphi_i\rangle\langle\varphi_i| \quad (1.18)$$

Where $|\varphi\rangle$ is orthonormal vectors.

And the trace of density matrix is equal to one [19]

$$Tr(\rho) = 1 \quad (1.19)$$

The trace is a linear map, which has properties [19]

- for square matrices A and B

$$Tr(A + B) = Tr(A) + Tr(B) \quad (1.20)$$

$$Tr(sA) = sTr(A) \quad (1.21)$$

Where *s* is a scalar.

One more formula is when matrix A with *(m × n)* and matrix B with *(n × m)* so [19],

$$Tr(AB) = Tr(BA) \quad (1.22)$$

Finally, the trace of a matrix A equal to the trace of its transpose A^T are as shown below[19]:

$$Tr(A) = Tr(A^T) \quad (1.23)$$

The conjugate transpose of the *m × n* matrix A *is* A*, so[19]

$$Tr(A^*A) \geq 0 \quad (1.24)$$

The inner product is used to find the angle between the two vectors as ⟨A, B⟩ = *Tr* (B*A). If the inner product of the two vectors is zero, then the vectors are orthogonal. Also the trace operation helps to distinguish pure and mixed state [19].

1.3.7 Pure and mixed quantum state

When a system has mixture of states $|\varphi\rangle_i$ with probability p_i, the system can be shown as density matrix [18]:

$$\bar{\rho} = \sum p_i |\varphi\rangle_i \langle\varphi|_i \quad (1.25)$$

The quantum system whose state $|\varphi\rangle_i$ is known exactly it will be in a pure state. So the density operator is simply expressed as [18]:

$$\rho = |\varphi\rangle\langle\varphi| \quad (1.26)$$

Otherwise, the system is a mixed state, when the system is a mixture of different pure states. So, to identify the state of system that represented by density matrix, pure states have the property $Tr(\rho^2)$ =1, while for mixed states $Tr\ (\rho)^2 < 1$ [18].

1.3.8 Composite systems

Quantum states that live in different Hilbert spaces can be combined by using the tensor product to produce the Hilbert spaces. The tensor product is a mathematical tool that acts on the Hilbert spaces to create a composite system H_{AB} as $H_A \otimes H_B$. The dimension of the combined Hilbert space N_{AB} is $N_{AB} = |N_A| * |N_B|$, the product of the dimensions of the original spaces. To write the composition of quantum states, product states must be applied by a tensor product form between states.

Consider two general qubits are [18]:

$$|\varphi\rangle_A = \alpha|0\rangle_A + \beta\,|1\rangle_A$$

$$|\varphi\rangle_B = a|0\rangle_B + \mathrm{b}\,|1\rangle_B$$

The product state of these two qubits is given by [18]:

$$|\varphi\rangle_A \otimes |\varphi\rangle_B = (\alpha|0\rangle_A + \beta\,|1\rangle_A) \otimes (a|0\rangle_B + \mathrm{b}\,|1\rangle_B) \qquad (1.27)$$

This can be expanded with the tensor product as [18]:

$$|\varphi\rangle_{AB} = \alpha a|0\rangle_A|0\rangle_B + \alpha b|0\rangle_A|1\rangle_B + \beta a|1\rangle_A|0\rangle_B + \beta b|1\rangle_A|1\rangle_B \qquad (1.28)$$

Each system is completely uncorrelated from the other, implying that system A(B) cannot know any information about the system B(A) just based on local operations or measurements. Unless states are not isolated and interact with each other, they may become entangled. States that cannot be factored in the form of a tensor product are considered entangled. Entangled states are a more generalized combined state, in the sense that there are no restrictions on the factorability of the coefficients in (1.27) to form a product state [18].

1.3.9 Quantum Gates

Changes can occur to a quantum state by utilizing the language of quantum computation [17]. This computation can be done by the quantum gates as seen in the classical computation which is done by the classical gates. Density matrices are utilized to describe the quantum gates [18, 19]. Quantum logic gates are reversible while the classical logic gates aren't. There are many types of quantum gates according to the input quantum state such as single qubit and multiple qubits quantum gates. The single qubit gates are:

- **Pauli-X or bit-flip gate**

This gate exchanges the amplitudes of computational basis states , as shown below [17]

$$|\varphi\rangle = X|\emptyset\rangle = \begin{bmatrix}0 & 1\\ 1 & 0\end{bmatrix}\begin{bmatrix}a\\ b\end{bmatrix} = \begin{bmatrix}b\\ \mathrm{a}\end{bmatrix} \equiv b|0\rangle + a|1\rangle \quad (1.29)$$

- **Pauli-Z or phase-flip gate**

This gate flips the phase of second amplitude by 180^0 [17]

$$|\varphi\rangle = Z|\emptyset\rangle = \begin{bmatrix}1 & 0\\ 0 & -1\end{bmatrix}\begin{bmatrix}a\\ b\end{bmatrix} = \begin{bmatrix}a\\ -b\end{bmatrix} \equiv a|0\rangle - b|1\rangle \quad (1.30)$$

- **Pauli-Y gate**

This gate makes (π / 2) phase shift between the initial and final state [17]

$$|\varphi\rangle = Y|\emptyset\rangle = \begin{bmatrix}0 & -j\\ j & 0\end{bmatrix}\begin{bmatrix}a\\ b\end{bmatrix} = \begin{bmatrix}-jb\\ ja\end{bmatrix} \equiv -jb|0\rangle + ja|1\rangle \quad (1.31)$$

- **Phase-rotator or phase gate**

Phase gate makes rotation to the probability amplitude of computational basis state$|1\rangle$ by an angle α [17]:

$$|\varphi\rangle = P|\emptyset\rangle = \begin{bmatrix}1 & 0\\ 0 & e^{j\alpha}\end{bmatrix}\begin{bmatrix}a\\ b\end{bmatrix} = \begin{bmatrix}a\\ be^{j\alpha}\end{bmatrix} \equiv a|0\rangle + be^{j\alpha}|1\rangle \quad (1.32)$$

- **Hadamard gate (H gate)**

  H gate impacts on the qubit as shown below [17]:

$$H|0\rangle \rightarrow \frac{|0\rangle+|1\rangle}{\sqrt{2}} \quad (1.33)$$

$$H|1\rangle \rightarrow \frac{|0\rangle-|1\rangle}{\sqrt{2}} \quad (1.34)$$

  These show the state $|0\rangle$ and $|1\rangle$ have equal probabilities of measurement.

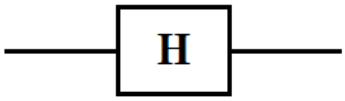

Figure 1.1: The circuit representation of Hadmard gate [17]

The multiple qubit quantum gates are:

- **The Controlled- Not gate**

  These gates act on two or more than one qubits, in which at least one qubits work as a control. The most significant type of such gates is the controlled- Not gate (CNOT or CX), which has two input qubits, the first one is called the control qubit and the other is the target qubit, If the first qubit is $|1\rangle$, then NOT operation performed on second qubit, otherwise nothing is done. The circuit that represents the CNOT gate is shown below [17]:

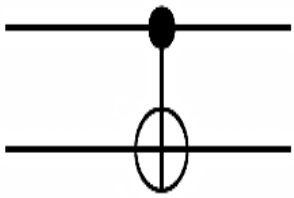

Figure 1.2: The circuit representation of the CNOT gate [17]

- **The Toffoli gate**

This gate is a three-qubit gate utilized for classical computation. The Toffoli gate mechanism is when the first two qubits are in state, then a Pauli-X (or NOT) is performed on the third bit, otherwise it does nothing. The Toffoli gate can be considered like the quantum analog of a classical gate. The circuit of Toffoli gate is shown below [17].

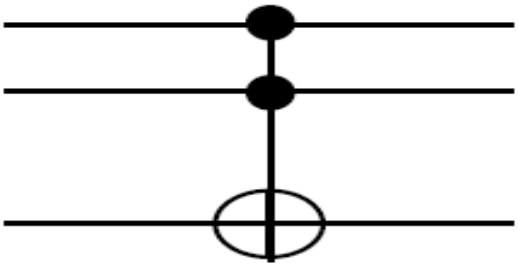

Figure(1.3): The circuit representation of the Toffoli gate

1.3.10 Quantum entanglement

Unlike the classical system, the quantum system exhibits a unique phenomenon that happens when a pair of particles is created; they interact in particular way so that the quantum state of the first particle can't be defined independently of the state of the second one, even though the particles are separated by a huge distance. Entangled particles are found to be absolutely related to measurements of physical proprieties like momentum, spin position, and polarization. As an example, if a pair of particles is formed and their total spins is zero, so the first particle will have clockwise spin on a certain axis, and the other particle will have counterclockwise spin on the same axis, this happen because of their entanglement [19]. An example of entangled states is Bell states (EPR) which shown in (1.35). The term EPR refers to the physicists Einstein, Podolsky, and Rosen who were the first discovered the entanglement states

and the fundamental representation of the two particles in a maximally entangled state [17]

$$|\Phi^+\rangle = \frac{1}{\sqrt{2}}(|00\rangle + |11\rangle)$$

$$|\Phi^-\rangle = \frac{1}{\sqrt{2}}(|00\rangle - |11\rangle)$$

$$|\Psi^+\rangle = \frac{1}{\sqrt{2}}(|01\rangle + |10\rangle) \qquad (1.35)$$

$$|\Psi^-\rangle = \frac{1}{\sqrt{2}}(|01\rangle - |10\rangle)$$

The Bell states form an orthonormal basis in four dimensional Hilbert space and are very important tool in quantum information. Any measurement performed on this basis is referring to as Bell state measurement. The circuit that creates the Bell states is consists of Hadmard gate and C-Not gate as shown in Figure (1.4)

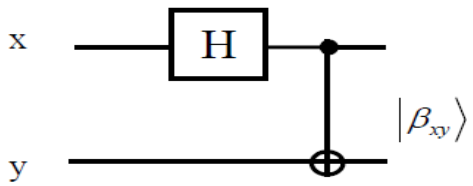

Figure (1.4): Bell state creation circuit [18]

1.3.11 No-Cloning theorem

The theorem of no-cloning was stated in 1982. It effects on the quantum mechanism .The no cloning theorem prevents the creation of indistinguishable copies of random unidentified qubit, also it has many consequences in quantum communications and related fields. No-Cloning theorem is important for the security of quantum communication protocols and quantum teleportation for transmitting of quantum information. This

problem is overcome by using the quantum repeater which exchanges the entangled states between Alice and Bob [20].

1.4 Quantum communication

1.4.1 Superdense coding

The information theory is the science that investigates the theoretical limits of communication over an erroneous channel. One of the examples on the information theory is the superdense coding which was proposed by Bennett and Wiesner in 1992 [21].

The superdense coding can be explained when Alice and Bob exchange the information between each other over an error-free quantum channel and use the superdense code. The major steps presented in the following steps [17]

1- Alice and Bob prepare several Bell states $|\beta_{00}\rangle$ that are equal to $|\beta 00\rangle = |00\rangle + |11\rangle/\sqrt{2}$ and each of Alice and Bob will have one qubit of each pair.

2- Then Alice makes conversion on the speech signal to classical bits 0s and1s.

3- Next she uses the coding rules in the first two columns of Table (1.1) on the half pair and encodes each pair of two consecutive bits into a superposition state. Then Alice sends her qubit to Bob over the quantum channel.

4- Now Bob receives the qubit and restores the original classical information by decoding. He calculates the possible joint states of the two-qubit system and records them in the third column of Table (1.1).

Table 1.1: the encoding rules [17]

Dibit	transform	Joint state
00	I	$\frac{\|00\rangle + \|11\rangle}{\sqrt{2}}$
01	Z	$\frac{\|00\rangle - \|11\rangle}{\sqrt{2}}$
10	X	$\frac{\|10\rangle + \|01\rangle}{\sqrt{2}}$
11	jY	$\frac{\|01\rangle - \|10\rangle}{\sqrt{2}}$

5- Classical inputs can be achieved from the outputs, by implementing Hadamard and CNOT gates. Because of the unitary property of the Bell gate. It's inverse can be calculated as its adjoint

$$((H \otimes I)\,CNOT)^{-1} = ((H \otimes I)\,CNOT)^{\dagger} = CNOT^{\dagger}\,(H \otimes I)^{\dagger} \quad (1.36)$$

Both (H ⊗ I) and CNOT are Hermitian operators. When Bob receives the qubits, he decodes them by implementing these gates in reverse manner to construct the decoder.

This algorithm is called superdense coding because only half amount of qubits has to be sent.

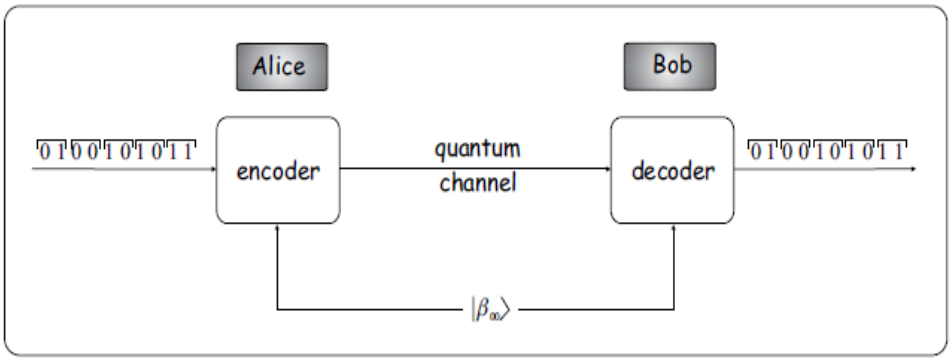

Figure 1.5: The superdense coding [17]

1.4.2 Quantum teleportation

When Alice and Bob share an entangled state, then Alice (Bob) transfers an unknown quantum state to Bob (Alice) without actually moving the unknown state through a process called the quantum teleportation. The first theory of quantum teleportation was represented by Charles Bennett and his international team in 1993[22]. Figure (1.6) shows the operation of the teleporting device.

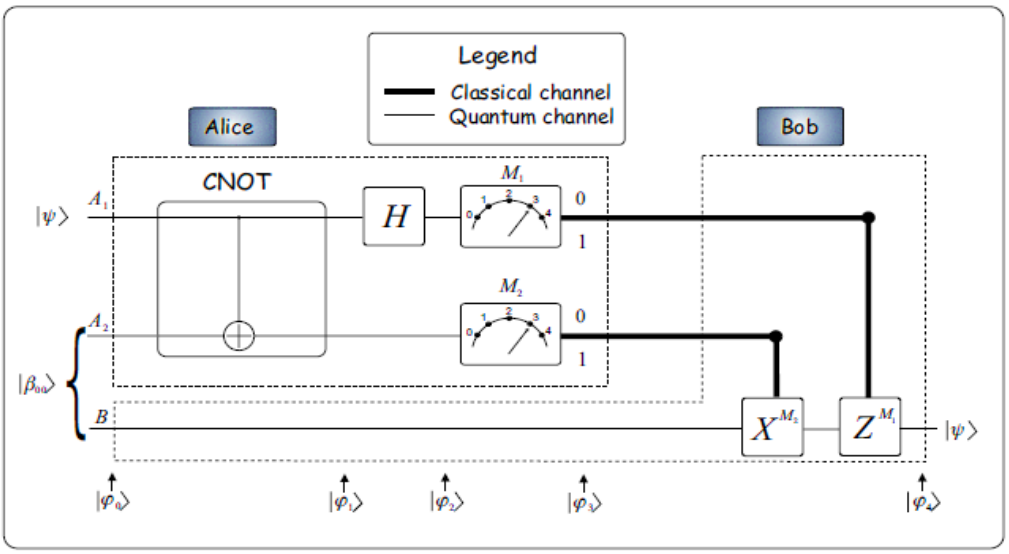

Figure (1.6): procedure of teleportation [17]

Suppose an arbitrary quantum state $|\varphi\rangle$ of a particle needs to be teleported, where

$$|\varphi\rangle = a|0\rangle + b|1\rangle$$

First, Alice and Bob share a $|\beta 00\rangle = |00\rangle + |11\rangle/\sqrt{2}$ Bell pair, where Alice quantum wires is A_1 and A_2 and Bob's half pair wire is B. So the initial joint state is [17]

$$|\varphi_0\rangle = |\psi\rangle|\beta_{00}\rangle = \frac{1}{\sqrt{2}}\left[a|0\rangle^{A_1}\left(|0\,0\rangle^{A_2B} + |1\,1\rangle^{A_2B}\right) + b|1\rangle^{A_1}\left(|0\,0\rangle^{A_2B} + |1\,1\rangle^{A_2B}\right)\right] \quad (1.37)$$

Next Alice performs a CNOT gate onto the qubits, so the state will be [17]

$$|\varphi_1\rangle = \frac{1}{\sqrt{2}}\left[a|\overset{A_1}{0}\rangle\left(|\overset{A_2B}{0\,0}\rangle + |\overset{A_2B}{1\,1}\rangle\right) + b|\overset{A_1}{1}\rangle\left(|\overset{A_2B}{1\,0}\rangle + |\overset{A_2B}{0\,1}\rangle\right)\right]. \quad (1.38)$$

Then, Hadamard transform on the top quantum wire is applied. The Hadamard rule is shown in (1.33), (1.34), this leads to [17]

$$|\varphi_2\rangle = \frac{1}{\sqrt{2}}\frac{1}{\sqrt{2}} \times \left[a\left(|\overset{A_1}{0}\rangle + |\overset{A_1}{1}\rangle\right)\left(|\overset{A_2B}{0\,0}\rangle + |\overset{A_2B}{1\,1}\rangle\right) + b\left(|\overset{A_1}{0}\rangle - |\overset{A_1}{1}\rangle\right)\left(|\overset{A_2B}{1\,0}\rangle + |\overset{A_2B}{0\,1}\rangle\right)\right] \quad (1.39)$$

Alice rearranges $|\varphi_2\rangle$ according to her two qbits to produce a readable form [17]

$$|\varphi_2\rangle = \frac{1}{2}\left[|\overset{A_1A_2}{0\;0}\rangle\left(a|\overset{B}{0}\rangle + b|\overset{B}{1}\rangle\right) + |\overset{A_1A_2}{0\;1}\rangle\left(a|\overset{B}{1}\rangle + b|\overset{B}{0}\rangle\right) + |\overset{A_1A_2}{1\;0}\rangle\left(a|\overset{B}{0}\rangle - b|\overset{B}{1}\rangle\right) + |\overset{A_1A_2}{1\;1}\rangle\left(a|\overset{B}{1}\rangle - b|\overset{B}{0}\rangle\right)\right] \quad (1.40)$$

Clearly, the measurement outcome of Alice will be one of the four possible two-bit results among 00, 01, 10 or 11, and then she sends these two classical bits to Bob who will compare $|\varphi\rangle$ to the potential states of his half Bell pair as shown in the following relations [17]

$$\begin{aligned} A_1A_2 \rightarrow \quad B \quad &= U|\varphi\rangle \\ 00 \rightarrow \frac{a|0\rangle + b|1\rangle}{2} &= I|\varphi\rangle \\ 01 \rightarrow \frac{a|1\rangle + b|0\rangle}{2} &= X|\varphi\rangle \\ 10 \rightarrow \frac{a|0\rangle - b|1\rangle}{2} &= Z|\varphi\rangle \\ 11 \rightarrow \frac{a|1\rangle - b|0\rangle}{2} &= ZX|\varphi\rangle \end{aligned} \quad (1.41)$$

According to the relations in (1.41), Bob will implement the opposite of the transform(s) in keeping with the received classical bits. All operators are unitary, so the inverses of them can be obtained by building their adjoint. Also, they are Hermitian which explains why the original gates are controlled by measurement results M_1 and M_2 so, that help Bob to get his original state $|\varphi\rangle$.

1.4.3 Entanglement swapping

Entanglement swapping is based on the same theory as quantum teleportation, but there is Charlie whose position is between Alice and Bob. If Alice and Charlie, Bob and Charlie, share entangled state, for instance a maximally entangled Bell state, then Charlie can perform a Bell state measurement on his two qubit states [23].

Table 1.2: The operations of Bob [50]

Bell state measurement outcome	Bob's operation
$\|\emptyset^+\rangle$	Do nothing
$\|\emptyset^-\rangle$	Phase flip
$\|\varphi^+\rangle$	Bit flip
$\|\varphi^-\rangle$	Bit and phase flip

This leads to that Alice and Bob share an entangled bipartite. After Charlie performing a Bell state measurement, he reports his measurement results to Bob or Alice to fix their state with the same operations as the quantum teleportation scheme utilized in Table (1.2). The entanglement swapping used for many quantum repeater schemes to allow the generation of entanglement between two parties who spatially separated [23].

1.4.4 Quantum key distribution

Quantum key distribution (QKD) is a secure protocol where private bits can be made between points spatially separated and linked via public channel. The aim of QKD is to transfer the quantum information over a public channel with an error less than precise limit [18]. The BB84 protocol is one of the most popular protocols, which was invented in 1984 by Charles Bennett and Gilles Brassard [24]. The essential idea of this protocol is that Alice sends a sequence of photons to Bob which are encoded in their polarization. According to Heisenberg's Uncertainty Principle, Eavesdropper disturbs the photon's state in a detectable way so that will expos her existence if she measures these photons and transmit them to Bob. In BB84 protocol the information bit has encoded in the polarization state of a photon. A binary 0 is defined as the polarization of 0 degrees in the rectilinear bases or 45 degrees in the diagonal bases [25] [26]. A binary 1 is also identified as 90 degrees in the rectilinear bases or 135 in diagonal bases. So a bit can be interpreted by polarizing the photon in any one of two bases as shown in Figure (1.7).

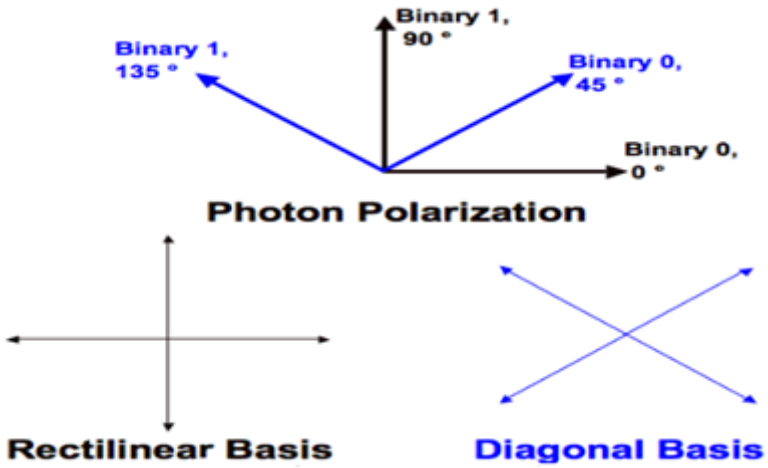

Figure 1.7: BB84 Bit Encoding [25]

1- At the beginning, Alice will link to Bob via a quantum channel. Alice selects a random string of bits then she chooses a rectilinear basis or diagonal basis to encode each bit. After that, Alice will transmit a photon with the corresponding polarization for each bit.
2- Bob receives the photons and measures their polarization by selecting a basis randomly.
3- Steps 1 and 2 are repeated for a large numbers of times to obtain random bit string which is called the raw key.
4- Using the authenticated channel, Alice and Bob tell to each other the basis they used to send and measure each photon.
5- Each of Alice and Bob will cancel the bits which Bob measured in a different basis, because Alice and Bob should have the same string of bits which is called a sifted key. The example below in Figure (1.8) shows the bits Alice chose, the bases she encoded them with the bases Bob used for measurement and the resulting sifted key after Bob and Alice discarded their bits.

Alice's bit	0	1	1	0	1	0	0	1
Alice's basis	+	+	X	+	X	X	X	+
Alice's polarization	↑	→	↖	↑	↖	↗	↗	→
Bob's basis	+	X	X	X	+	X	+	+
Bob's measurement	↑	↗	↖	↗	→	↗	→	→
Public discussion								
Shared Secret key	0		1			0		1

Figure1.8: an example of the bits of Alice and the bases that she used to encode them, the Bob used for measure and the sifted key [25]

Finally, Alice and Bob compare subset of the bits to ensure consistency.

1.4.5 Secret key rate

The secret key rate is the most important figure of merit to evaluate the quantum key distribution protocol. The secret key rate per channel use is the number of bits of secret key that can be produced each time of using the quantum channel, when the infinitely long secret key is limited. The secret key rate for efficient BB84 when using a single photon is [27, 28]

$$R = Y_1[1 - h(e_1) - fh(e_2)] \qquad (1.42)$$

Here Y_1 is the yield which is the probability of Bob when makes a successful detection of photon that Alice sent. e_1 is the quantum bit error rate (QBER) which is the fraction of Alice and Bob's sifted bits that don't match, and the factor f is an error correction inefficiency factor, which is equal to 1 in the ideal error correction scheme and in non–ideal scheme has f >1. Finally, the fraction h is binary entropy function which is equal to:

$$h(x) = -\mathrm{x}log_2(x) - (1 - \mathrm{x})log_2(1 - x) \qquad (1.43)$$

1.4.6 Quantum repeaters

The direct transmission of photons between two spatially separated points is difficult due to the exponential loss of propagation. In order to pass this obstacle, intermediate stations are used between the two distant points. These stations are known as a quantum repeater (QR). The idea was presented in 1998 by H. J. Briegel et al. [29],who proposed a quantum repeater protocol to setup entanglement between two isolated destinations by performing entanglement swapping, entanglement purification, and quantum memory [29,30]

Principle of a QR is represented in Figure (1.9). The channel is divided to many sections and connected by quantum repeaters to establish the

entanglement between neighboring sections. The entanglement that could be established between the closest sites can be expanded by implementing the entanglement swapping to increase the communication channel length. But, the entanglement swapping isn't perfect and the fidelity of entanglement will decrease after a couple of association steps, so the entanglement purification was used to enhance the quality of entangled pairs [31, 32].

A nested purification scheme appears in Figure (1.9), the entanglement swapping and entanglement purification is repeated many times until a remote entangled pair with high fidelity is formed between the two distant stations. It was shown that time overhead and sources needed to establish the remote entangled pair is related polynomially to the distance [33]. The QR consists of two quantum memories to store the state space and Bell state measurement between them to measure the states.

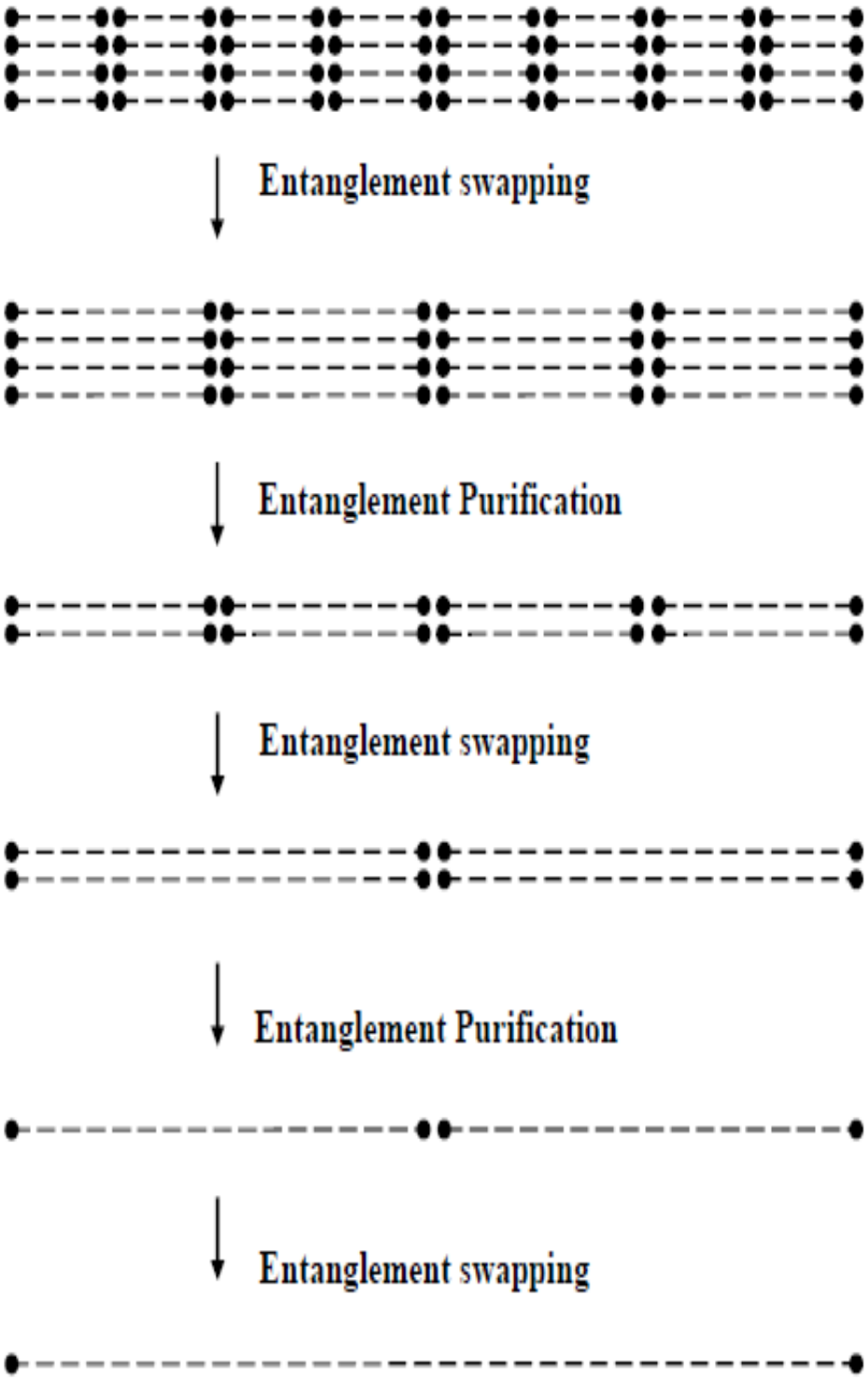

Figure 1.9: Quantum repeater protocol where the entanglement swapping is used to expand the channel, while the entanglement purification is used to enhance the fidelity of entangled pair [32]

1.4.6.1 Quantum memories

Quantum memory (QM) is an important part that plays a significant rule in many of quantum repeater schemes which is capable of storing intermediate quantum states between links. The quantum memory is defined as any physical system that can write, store and reads out the quantum state [34]

In the QR protocol [14], the communication channel is divided into many links with lengths comparable with communication channel attenuation length. Entanglement is then produced and purified for each link before it is distributed over a longer distance by an entanglement swapping process. Consequently, a teleportation of quantum data can be achieved. Due to the probabilistic nature of the purification [34, 39] and the need of storing the already successful states in quantum memory while waiting for the others, quantum memory with long storage time is vital to accomplish scalable quantum communication systems [36]. Physical implementation requires a light matter interface, as photonic states are read in, stored in matter and read out as photonic states. Some types of quantum memories may produce photonic states entangled by a state stored in the QM via some control mechanism. The performance of the QM can be estimated by the preparation efficiency, preparation time of generating a memory photon entangled state, the wave length of emitted photons, the efficiency of coupling the photon into fiber and the decoherence time of the stored state. If QMs are introduced in a communication channel, the decoherence time must be greater than the communication time to minimize errors. In fact, the frequency of the emitted photon is important because the dispersion and attenuation of photons in fiber are dependent on wavelength, the lowest fiber attenuation wavelength for telecommunication is around 1550 nm [35].The wavelength of the photon that is emitted from the QM depends on the type of QM, e.g. the quantum dots have a photon emission wavelength

around 1.37μm [36]. In order to match the wavelength of photons generated by the QMs with low loss optical fiber, a conversion of the wave length must be done before transmission. There are number of proposed and demonstrated types of QMs like, Nitrogen- Vacancy (NV) center and the trapped ion QMs.

- **Nitrogen- Vacancy center quantum memory**

Nitrogen- Vacancy (NV) center is a point defect in diamond with $C3v$ symmetry, which consists of a pair formed between a substituted nitrogen atom in diamond and a lattice vacancy [34]. The reason of success of diamond defect and use it in the quantum technology is due to: first, is the narrow optical emission and excitation lines, also the stable room temperature because of the diamond color centers are defected in the diamond band. The second is the long of the electron and nuclear spin dephasing time due to the fact that the stiff and diamagnetic diamond lattice, as an example it can reach millisecond for electron spin at T=300K. The NV -center has number of properties that makes it an interesting system for quantum memory [37, 38]

1. A bright, photo stable optical transition which used as a source of single photons.
2. A magnetically resonant and controllable spin-state with long coherence times (long $T2$ approaching $\sim$ 1 second)
3. Ability to optically spin-polarize and to readout the spin optically.

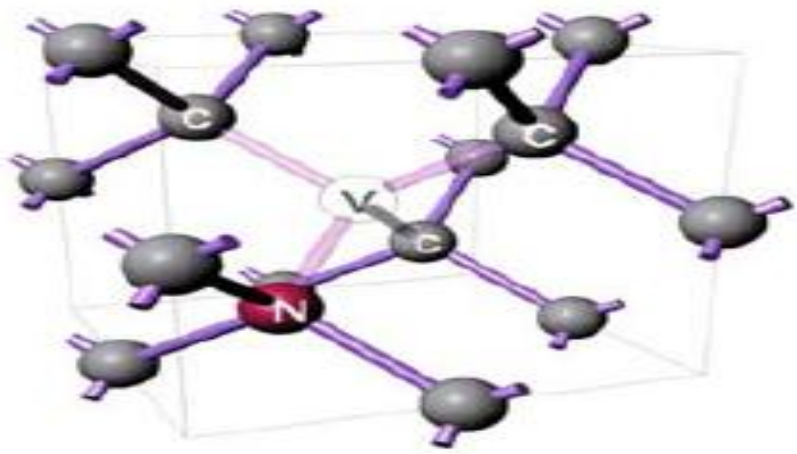

Figure 1.10: schematic of the NV-center embedded in the diamond lattice [37]

At low temperature, NV center enables optical excitation and emission line width of around 10 MHz. This will lead to good cavity coupling in order to optimize the interface of spin photon [39]. The absorption wavelength range is from ultraviolet to infrared and long coherence times. The emission wavelength of NV center is around 700 nm which is not in the telecommunication range. Longer wavelength can be achieved by using different defect centers. NV-center is a popular platform for a number of landmark demonstrations in quantum information science, like room temperature demonstrations of quantum registers [40], spin-photon entanglement [41], loophole-free Bell tests [42], and quantum cryptography [43].

- **Trapped ion quantum memory**

Trapped ion is a quantum memory that can be achieved by confining the ions or charged particles in free space by applying electromagnetic fields. The Trapped ion can store quantum bits in stable electronic states. Also the ions are used to send the quantum information through the shared trap. The lasers are used to make the coupling between the qubit states for single qubit operations also for the entanglement by

making the coupling between the qubit states and motional states [18]. In trapped ion quantum computing experiments, the electro dynamic ion trap which is shown in Figure (1.11) is commonly used which was invented by Wolfgang Paul in 1950 [46]. The idea is based on using an electric field oscillating at radio frequency (RF) to trap the charged particles in 3D. The oscillation frequency and field strength of the RF field makes the charged particle trapped at the saddle point which is a point of minimized energy magnitude |E(x)| for the ions in the potential field [45]. The Paul trap traps the ions in just two dimensions assuming they are x and z but in y direction the ions can move if they are at the saddle point and the system is at balance. Therefore, the ions create a vertical configuration in y because they will repel each other [46]. Current studies are about creating a system that contains large amount of qubits and have the ability to transport the ions to far locations, like building large networks which connected photonically via remotely entangled ion. The number of particles to be controllably entangled is 20 trapped ions can be archived in April 2018.

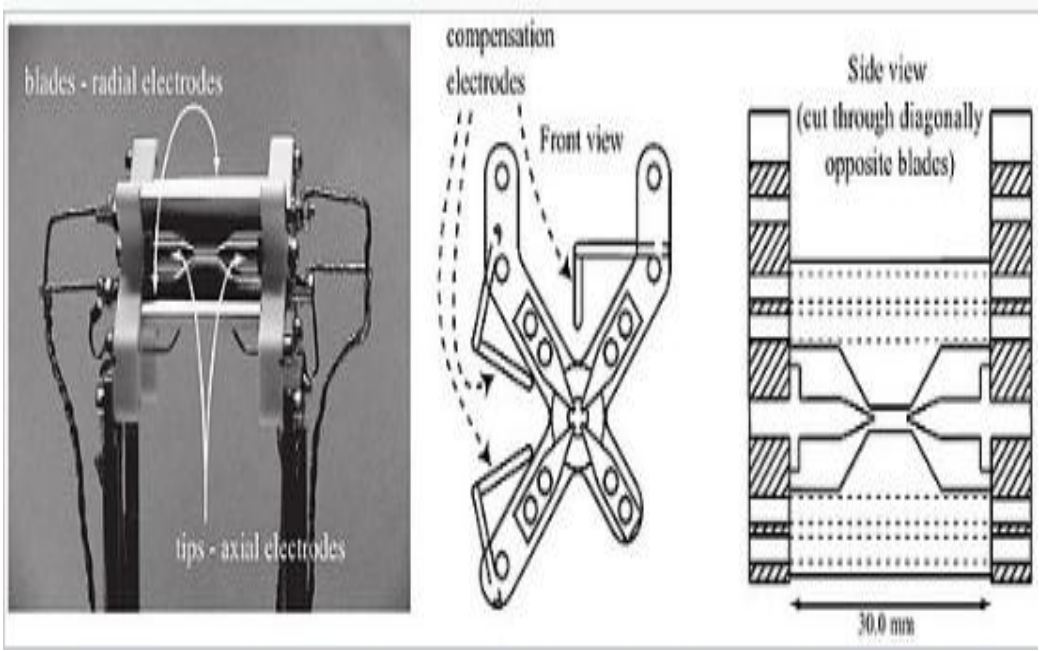

Figure1.11: Classical linear Paul trap [46]

1.4.6.2 Bell state measurement

The four Bell states in equations (1.35) can be distinguished by Bell state measurement which uses beam splitters and single photon detectors as shown in Figure (1.12). Bell state measurement can be used in every node of quantum repeater for creating the entanglement between each two elementary links.

A Bell state measurement is a joint measurement on two qubits, which projects a qubits onto one of the Bell states [47].

Figure 1.12: Bell state measurement [47]

1.4.7 Frequency conversion

This is an important feature of quantum communication because it gives the ability to control the optical frequency of the quantum state carriers like photons. This technique allows the quantum systems to be compatible with telecommunication C band, where at this band the fiber losses are the lowest, since this will enable long distance fiber quantum communication between Alice and Bob. The general frequency conversion process (FC) is shown in Figure (1.13) [48]. A strong pump beam with two input beams $\hat{a}$ (in) and $\hat{c}$ (in) enter a nonlinear crystal which transform them into two output fields $\hat{a}$ (out) and $\hat{c}$ (out). The input beam is combined with the pump beam to generate an output field either at a higher

frequency $\omega_{out} = \omega_{in} + \omega_p$ as shown in Figure (1.13)(a), this FC process is called sum frequency generation (SFG) ,or generate a field with frequency $\omega_{out} = \omega_{in} - \omega_p$ as shown in Figure (1.13)(b), which is called difference frequency generation (DFG).The difference between SFG and DFG arises by the input wave that is fed in either the $\hat{a}$ (in) or $\hat{c}$ (in) port. In the Figure (1.10) $\hat{a}$ (in) $\rightarrow$ $\hat{c}$ (out) describe a SFG process and $\hat{c}$ (in) $\rightarrow$ $\hat{a}$ (out) describe DFG. Usually any crystal configuration supports both processes simultaneously and the overall system is called frequency converter**.**

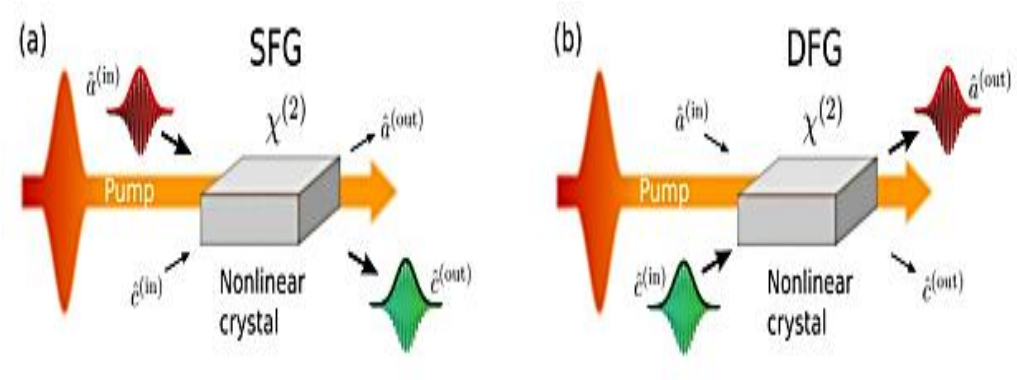

Figure 1.13: Frequency conversion process (a) SFG input filed converts $\hat{a}$ (in) to $\hat{c}$ (out), (b) DFG the filed $\hat{c}$ (in) converts to $\hat{a}$ (out) [48]

1.5 Literature survey

The previously proposed quantum repeater schemes which are related to the scheme presented in this work

In the following the most important research work in QR are reviewed:

(1) 2016 - D. Luong, L. Jiang, J. Kim, and N. Lutkenhaus. [49]

The Practical Realization of Quantum Repeaters: An Exploration Overcoming lossy channel bounds using a single node quantum repeater.

The study proposed a scheme for performing the quantum key distribution (QKD), which may beat schemes based on the direct transmission of photons between parties spatially separated.

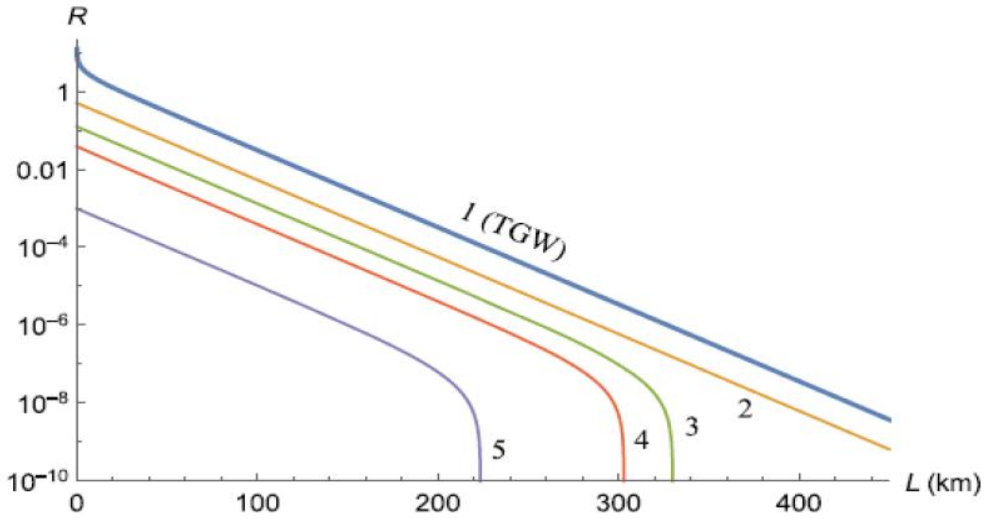

Figure 1.14: Key rate per channel vs. distance for different benchmarks

(2) 2017 - Christian Mastromattei [50]

Assessing the Practicality of a Simple Multi-node Quantum Repeater. The main aim of this study is to estimate the performance of specific multi-node quantum repeater, and compared with the performance of a single node repeater.

The results obtained showed rate versus distance scaling and it's relation with the number of nodes.

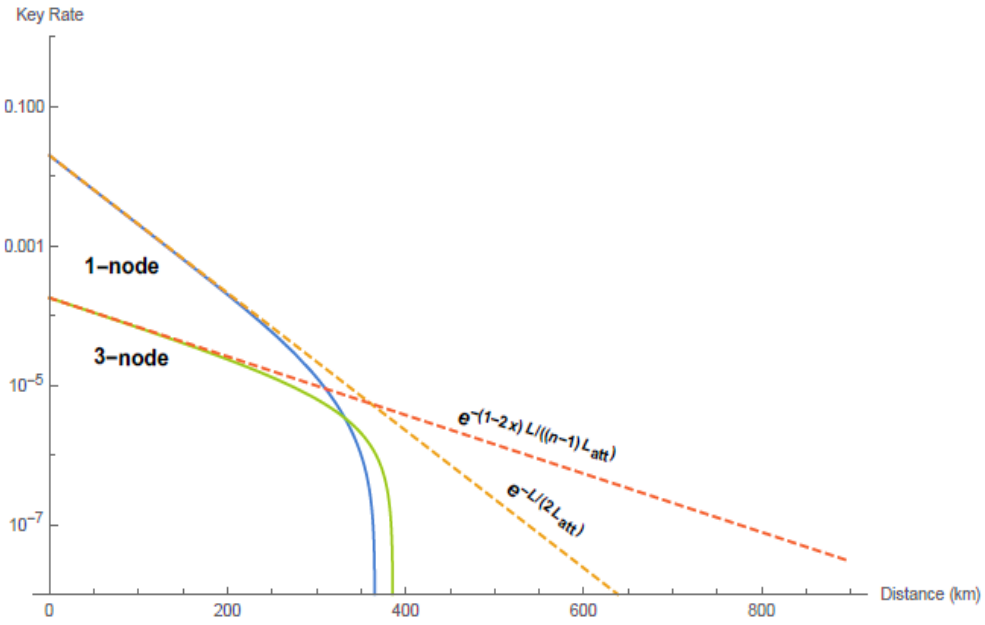

Figure 1.15: Key rates as a function of distance for one and three nodes

(3) Kadhim A.N., Hasan J.A. [51]

Analysis of a Quantum Repeater Scheme Based on Non-Identical Quantum Memories. The study analyze the performance of multi nod quantum repeater with non-identical quantum memories to optimize the rate between two distant points and increase the channel length as compared with repeater scheme based on identical quantum memories .

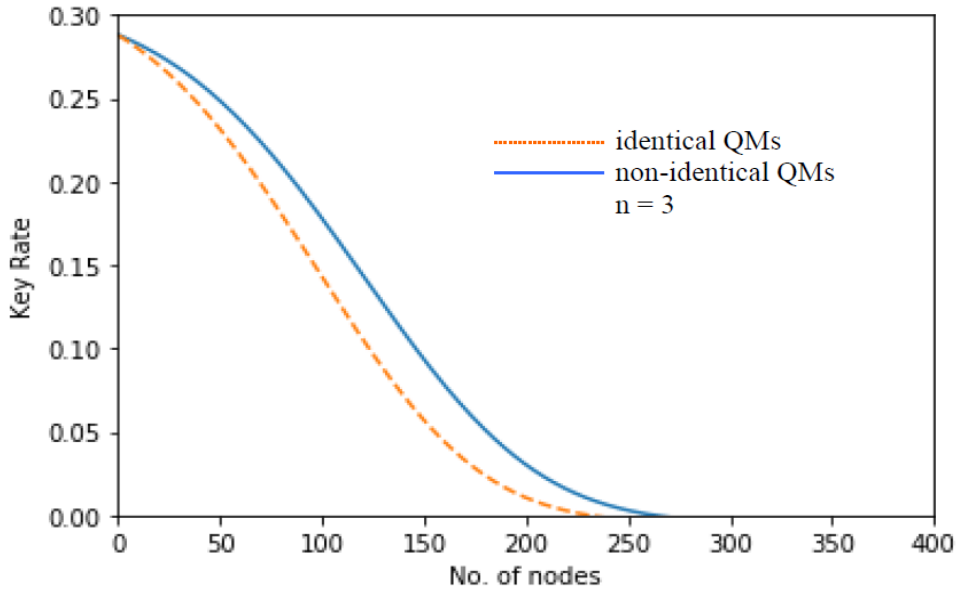

Figure 1.16: Key rate of identical QMs (dashed line) and non-identical QMs (bold line) when number of nodes = 3.

(4) 2017 - F. Rozpdek, et al. [14]

Parameter regimes for a single sequential quantum repeater. The study introduces the effect of cut-off on the performance of the QR. The concept reduces the effect of decoherence during storage of a quantum state by introducing a maximum storage time.

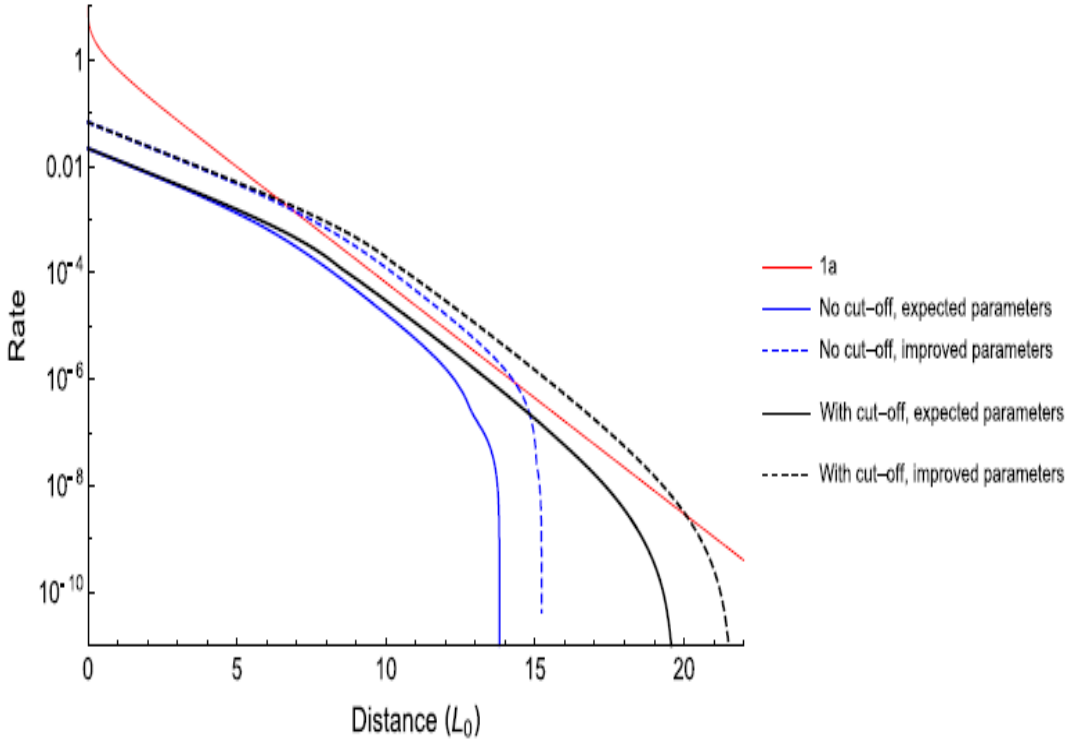

Figure 1.17: Secret key rate as a function of distance when Lo= 0.542 Km, without dark count

Chapter two
System Analysis

2.1 Introduction

The decoherence of the quantum state in the quantum memories is one of the problems that faces the quantum repeater, so a quantum repeater based on cut-off is one of the solutions to face this problem. To have the cut-off, the probability of Bob must be equal or greater than the probability of Alice in order to increase this probability quantum repeater with different quantum memories is proposed.

The effect of using different QMs on the performance of the quantum repeater is studied and its secret key rate is assessed by comparing it with the secret key rate of the quantum repeater based on the same types of quantum memories and direct transmission benchmark.

2.2 System Analysis

Quantum key distribution is the mature of the quantum technology in this time so; it is used to assess the performance of the quantum repeater [27].

The quantum repeater (QR) is a device that connects between two parties, Alice and Bob who are spatially separated and try to share a secret key between them. The basic idea of the quantum repeater is proposed in [49] which is the QR sends entangled photon with QM1 to Alice for many times until detection by BB84 measurement, then the QR sends entangled photon with QM2 to Bob for many times until detection by BB84 measurement when Bob detects the photon the BSM is applied. If Bob takes long time to detect the photon, the state in QM1 will be significantly decoheread this leads to prevent the generation of the secret key. So to avoid this, the QR

based on the cut-off was proposed in [16]. Which is the QR sends entangle photon with QM1 to Alice for many times until detection by BB84 measurement, then the QR sends entangle photon with QM2 to Bob for many times until detection by BB84 measurement is applied in specific number of trails (n*) if Bob makes BB84 measurement before n* the Bell state measurement is applied and if not the round will abort and start over again. This protocol reduces the decoherence of the quantum memories with time. In order to implement this protocol the probability of Bob must be equal or greater than the probability of Alice. In the original idea the probabilities of Alice and Bob are equal because of use the same quantum memories which they are Nitrogen Vacancy center, the equality of probabilities remains if any type of quantum memory is used because the quantum memories have the same values of parameters like the probability of emission and coupling. To make the probability of Bob greater than the probability of Alice, different QMs in the quantum repeater is proposed to get best n* and maximizing the secret key rate.

Fortunately, Entanglement between non-identical atoms is presented by two teams of researchers from University of Oxford and the other from the National Institute of Standards and Technology and the University of Washington [52, 53].

The team from University of Oxford [52] used two different isotopes of calcium, while the other team used beryllium and magnesium atoms [53]. The calcium atoms could keep their states for about a minute and about a second and a half for beryllium atoms.

Both teams stated that their two atoms are entangled with a very high probability in order of 0.998 for the first one and 0.979 for the second. So this project utilizes this achievement to enhance the system performance.

In this project the first QM is Nitrogen Vacancy center and the second is trapped ion, both of them have the ability to become entangled with a

photon. Alice and Bob are connected with the quantum repeater by optical fiber as shown in Figure (2.1).

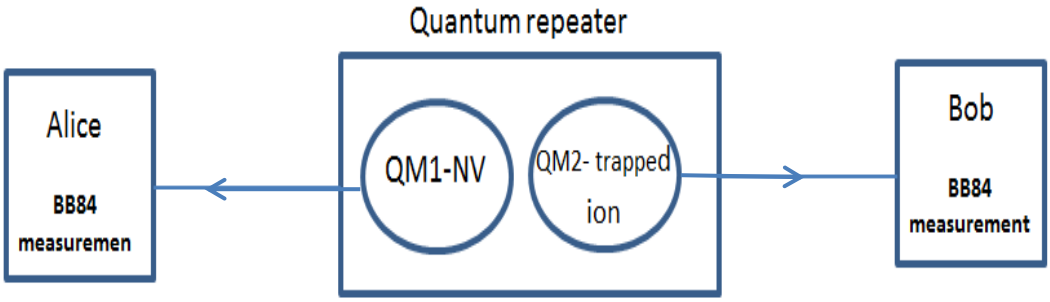

Figure (2.1): Schematic of the protocol. (QM1) sends entangled photons to Alice and makes BB84 measurement when she detects the photon, then (QM2) sends entangled photons to Bob and makes BB84 measurement when he detects the photon, then a Bell state measurement is performed on the QMs, if Bob doesn't detect the photon before n* the round will abort and start over again.

2.3 The protocol

In this protocol sequential quantum repeater is considered which is placed in the middle of the distance that separates Alice and Bob who want to create a secret key via QKD. The QM1 is Nitrogen-vacancy center (NV center) [54] which emits a single photon to Alice through an optical fiber with a transitivity δ_A and QM2 is a trapped ion [55]. The quantum repeater is coupled to an optical fiber with low attenuation of 0.1419 dB/km at wavelength of 1560nm [56] to achieve long distance, but Nitrogen-Nacancy center emits a single photon with a wave length of 637 nm [34] and the trapped ion emits a single photon with a wave length of 854 nm [57] so frequency conversion is needed to enhance the distance. Each of them had measurement apparatuses to measure the incoming photons in the x bases or in z bases, Alice and Bob decide the basis that they want to for measurement. It is as follows:

1- The NV center quantum memory prepares an entangled memory-photon state and sends one photon to Alice. The photons are continuously sent until Alice detects a photon and apply a BB84 measurement.
2- After that the trapped ion quantum memory prepares an entangled memory-photon state and sends the photon to Bob. If Bob doesn’t detect the photon with a specific number of trials (cut-off n*), the round will terminate and starts again.

3- If Bob succeeds before the cut-off, BSM is performed on the two quantum memories.

4- The classical outcome of the BSM is communicated to Bob.

5- This procedure is repeated to achieve appropriate amount of raw key.

2.4 Number of trails management

The number of trails effects the decoherence of state. When the number of trails is large, the state decohere so the reduce of this number enhance the key rate.

The use of different quantum memories decreases the number of n*that is needed to obtain the secret key rate because of the increment in the detection probability of photon in Bob's side

2.5 Sources of errors

Errors are identified by losses and noise. The system the losses come from the transmissivity of the optical fiber and from the lost photons before

coupling to the optical fiber or due to the non-unit detector efficiency. The noise is due to imperfections of the operations in the experiments as in measurements and quantum memories.

2.5.1 Losses in optical fiber

NV center and trapped ion quantum memories generate entangled photon with the quantum memory with emission probability of $p_{em/A}$, $p_{em/B}$. Then the photons entere the optical fiber but, only specific amount of photons enter the optical fiber can be used for secret key generation because they may be filtered according to frequency or a certain time window [58, 59] they are denoted by $p_{c/A}$, $p_{\mathrm{c/B}}$ for coupling NV center, trapped ion memory respectively.

In the optical fiber, the losses is an exponential decay of transmitivity

$$\delta = \mathrm{e}^{-\mathrm{L}/\mathrm{L_{att}}} \qquad (2.1)$$

For the optical fiber the attenuation length is $\mathrm{L_{att}}$. δ_{A} is denoted by the optical fiber losses on Alice's side and δ_{B} the optical fiber losses on Bob's side. Finally, the arriving photons will be captured by the detectors with efficiency p_{det}. This probability of detecting a photon will be increased by the presence of dark counts (which will also inevitably add noise to the system), the detectors of Alice and Bob are assumed to have the same detector efficiency and dark count.

2.5.2 Noise in the quantum repeater

The decoherence of the quantum state that is stored in quantum memory can be modeled by a decay of the fidelity with the number of trials n*. The reasons of decoherence in QMs are

1- The quantum repeater needs a time between successive photons sent. This time is taken to confirm whether the photon got lost or not. This model impact by an exponential decay of the fidelity with the time.
2- The QM2 needs time to generate an entangled photon-memory. This will decohere the state in the QM1. This model affects here an exponential decay of fidelity with the number of trials.

The quantum state, ρ, that is exposed with those impacts experiences a development given by the dephasing and depolarising channels with

$$\lambda_1 = (1 + e^{-an})/2 \quad (2.2)$$

$$\lambda_2 = e^{-bn} \quad (2.3)$$

Where $\lambda_1 = F_{prep}$ which is the dephasing parameter of preparation fidelity of memory photon entangled state and λ_2= is F_{gm} which it is depolarizing parameter that describes the noise introduced by imperfect gates and measurements between the different quantum memories. The two parameters a and b are given by:

$$a = a_0 + a_1 \left(\frac{2n_{ri} Lb}{c} + t_{prep}\right) \quad (2.4)$$

$$b = b_0 + b_1 \left(\frac{2n_{ri} Lb}{c} + t_{prep}\right) \quad (2.5)$$

- n_{ri}: Is the refractive index of the fiber, which is equal to 1.44 [60].
- c : is the speed of light in vacuum = $3*10^8$ m/sec
- Lb: is the distance from the quantum repeater to Bob
- t_{prep} : is the time that the trapped ion needs to prepare the emission of an entangled photon = 210 μs [61]

- a_0 and b_0 equal to the noise that come from to a single attempt of generating an entangled state where a_0 (NV) =1/2000 per attempt [62], b_0 (NV) =1/5000 per attempt [62];

- a_1 and b_1 quantify the noise during storage per second where a_1 (NV) =1/3 per second [63], b_1 (NV) =1/3 per second [63]

2.6 Secret key rate

The secret key rate (R) of equation (2.6) is used to assign the performance of scheme

$$\mathrm{R} = \frac{\mathrm{Y}}{2}\left(1 - h(ez) - h(ex)\right) \qquad (2.6)$$

The yield Y is the probability of Alice and Bob to detect a signal per round. $h(\mathrm{e})$ is the binary entropy function where

$$h(x) = -\mathrm{x}log_2(x) - (1-\mathrm{x})log_2(1-x) \qquad (2.7)$$

ex and ez are the quantum bit error rates (QBERs) between Alice and Bob in the x and z bases, and the factor of 1/2 comes from the fact that the protocol requires the use of two optical modes. The yield Y is inversely proportional with the number of channel use which is equal to [49]

$$\mathrm{Y} = \frac{P_{bsm}}{\mathrm{E}[\max(NA;NB)]} \qquad (2.8)$$

P_{bsm}: the probability of the Bell state measurement, NA is denoted by the number of the photons that need to be sent to Alice so that her detector clicks once and NB is denoted by the number of photons that need to be sent to Bob so that his detector clicks once. The average number of channel uses required for both Alice and Bob's detectors to click is $\mathrm{E}[\max(NA;NB)]$ where E is the expected value operator. The cut-off increases the average number of channel uses because when Bob reaches n* trials, Alice and Bob abort the round and start over again; therefore the expected value is [16]:

$$E[\max(N_A,N_B)] \approx \begin{cases} \frac{1}{P_A(1-(1-P_B)^{n^*})} & \frac{1}{P_A} > n^* \\ \frac{1}{P_A}+\frac{1}{P_B}-\frac{1}{P_A+P_B-P_AP_B} & \frac{1}{P_A} \le n^* \end{cases} \qquad (2.9)$$

When $\frac{1}{P_A} > n^*$is high loss regime where n* effect on the key rate while $\frac{1}{P_A} \leq n^*$ low losses regime is considered [49] where n* doesn't affect the secret key rate.

The analysis here depends on high loss regime to study the effect of n* on the secret key rate when useing two different memory. The probability of photon emitted from the NV center memory and detected by Alice can be denoted by P^*_A which is equal to:

$$P_A^* = P_{em/A} Fc_A \; P_{c/A} \delta_A P_{det} \quad (2.10)$$

And due to the dark count the probability of Alice will be:

$$P_{A,BB84} = 1 - (1 - P^*_A)(1 - P_d)^2 \quad (2.11)$$

Also, the probability that a photon emitted from the trapped ion and detected by Bob can be denoted by P^*_B which it is equal to:

$$P_B^* = P_{em/B} Fc_B \; P_{c/B} \delta_B P_{det} \quad (2.12)$$

And due to the dark count, the probability of Bob detector to click will be:

$$P_{B,BB84} = 1 - (1 - P^*_B)(1 - P_d)^2 \quad (2.13)$$

Where:

- $P_{c/A}$, $P_{c/B}$: probability of couplling quantum memory with fiber for Alice and Bob side respectively =0.46for NV center [58], = 0.4 for trapped ion [59]
- Fc_A : frequency conversion of the photon that emited from NV center memory = 0.3[64]
- Fc_B: frequency conversion of the photon that is emited from trapped ion memory = 0.5[65]

- δ_A : transmissivity of fiber that connects Alice with QR which is equal to $e^{-LA/L_{att}}$
- δ_B: transmissivity of fiber that connects Bob with QR which is equal to $e^{-LB/L_{att}}$
- L_{att} : the attenuation length of fiber which is = 22km [42]
- $P_{em/A}$: the probability of generating photon from NV into the optical fiber = 0.49 [42]
- $P_{em/B}$: the probability of generating photon from trapped ion into the optical fiber = 0.9[66].
- P_{det} : (detector efficiency) =0.8 the probability of photons to produce a click in the detector [42]
- p_d : is the probability of ganerating a dark count[42]
- bsm : BSM success probability [67]

2.7 Quantum bit error rates

The secret key fraction of the BB84 protocol is considered here .The expression for the secret key fraction depends on the error rates in the x, Y and z bases, which is denoted by e_x, e_Y and e_z.

$$e_x = e_Y = e_{xY} = 0.5 - 0.5\, F_{gm} \propto_A \propto_B \left(2F_{prep} - 1\right)^2 < e^{-(a+b)n} > \quad (2.14)$$

$$e_z = 0.5 - 0.5\, F_{gm} \propto_A \propto_B < e^{-bn} > \quad (2.15)$$

Where $\propto_A$, $\propto_B$ are depolarising parameters due to the noise that is achieved by the dark count at Alice's or Bob's detector respectively

$$\propto_{A,BB84} = \frac{\mathrm{P^*_A}(1-P_d)}{P_A} \quad (2.16)$$

$$\propto_{B,BB84} = \frac{P^*_B(1-P_d)}{P_B} \tag{2.17}$$

$$< e^{-cn} > = \frac{P_B \, \mathrm{e}^{-c}}{1-(1-P_B)^{n*}} \frac{1-(1-P_B)^{n*} e^{-cn}}{1-(1-P_B) e^{-c}} \tag{2.18}$$

Where $< e^{-cn} >$ is the average of the exponential e^{-cn} over a geometric distribution over the first n* trials.

2.8 Bench mark

To assign the secret key rate of the quantum repeater, it is compared with direct transmission benchmarks, because the quantum repeater is a source of additional losses. So, the first comparison of the protocol with a scheme based on the direct transmission of photons from Alice to Bob, is the Takeoka-Guha-Wilde (TGW) bound which is the most standard of comparison is. [68]

$$R_{TGW} = log_2\left(\frac{1+\delta}{1-\delta}\right) \tag{2.19}$$

Where = $e^{-L/L_{att}}$

Also, the protocol is compared with the secret key rate of direct transmission [49]. The transmissivity is equal to transmissivity of fiber, filters and Alice's and Bob's emission and detection probability, so it will become

$$\delta = \delta_{Fiber} \, P_{em} \, P_{det} \, P_c \, Fc \tag{2.20}$$

Chapter Three
Results and Discussion

3.1 Introduction

In this chapter, same and different quantum memories, performance and specifications, QR scheme performance, estimation of number of trails and their effect on key rate, and effect of QR position are calculated and discussed. The probability of detection and dark count are assumed to be the same for both Alice and Bob to estimate the effect of the quantum memories the on protocol. Python 3 is used for the programming of the calculations

3.2 Results:

Figure (3.1) shows the secret key rate of quantum repeater based on NV center for different number of n*. When n*= 5, 50 the secret key rate increases and the distance crosses 400Km, until n*is higher than 50 the losses increase and the secret key rate decays rapidly. This degradation in the secret key rate continues as long as n* increases. For different n*, It's still difficult to across the direct transmission bench mark

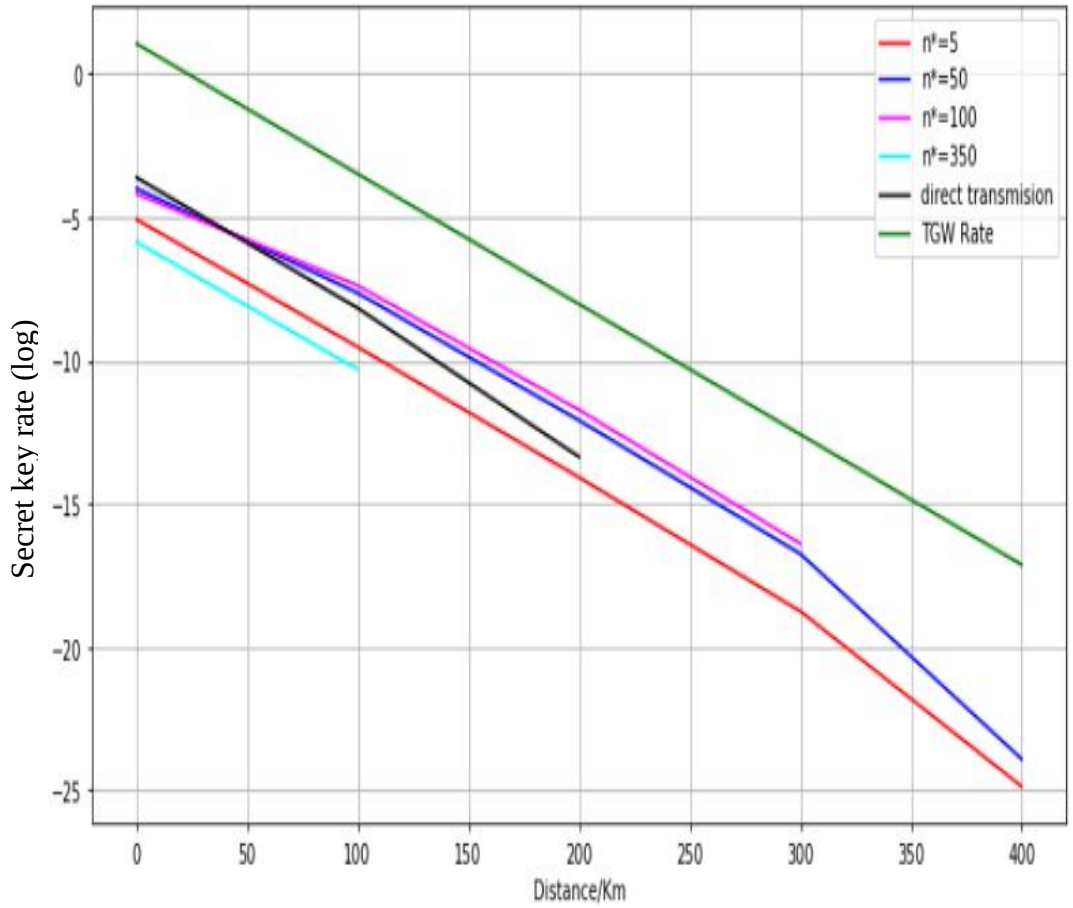

Figure 3.1: secret key rate of quantum repeater based on NV centre (probability of dark count= $3*10^{-7}$).

The probability of Bob may be increased by shifting the quantum repeater towards Bob. Figure (3.2) shows the effect of reducing the distance between Bob and the quantum repeater to increase the probability of detection. The secret key rate will decay rapidly when the quantum repeater is closer to Bob than Alice more than the secret key rate of the repeater when it is in middle of the distance that separate Alice and Bob at same n*.the figure shows that the best secret key rate can be achieved when the quantum repeater position is in the middle of the distance

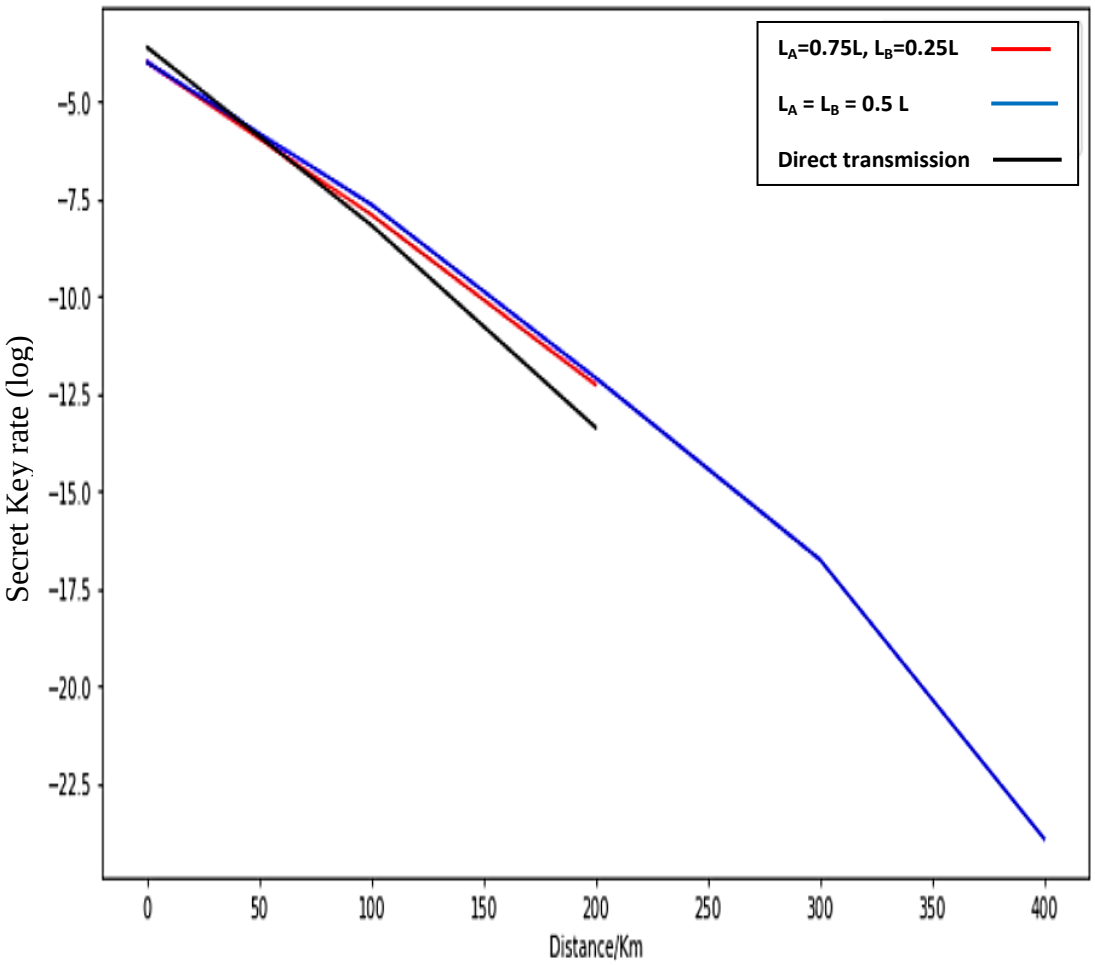

Figure 3.2: Different positions of quantum repeater based on NV center quantum memory when n*=50

In order to increase Bob's probability, the quantum repeater based on NV center-trapped ion is proposed. Figure (3.3) shows the enhancement of the protocol and an increase the secret key rate because the P_B is greater than P_A this will make efficient secret key rate but still difficult to across R_{TGW}

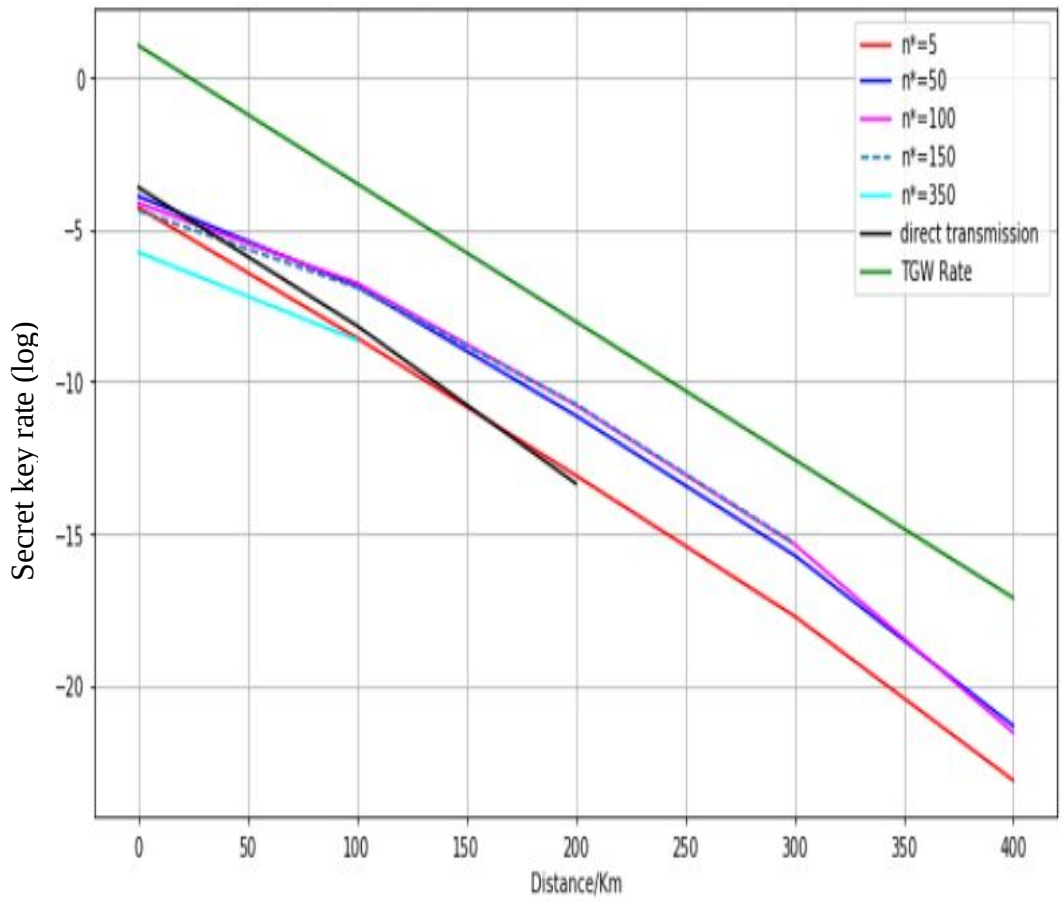

Figure 3.3: The secret key rate of quantum repeater based on NV centre -trapped ion (probability of dark count= $3*10^{-7}$).

Figure (3.4.a) shows achievement of higher secret key rate of quantum repeater based on NV center - trapped ion than a quantum repeater based on NV center. When n*=100 the secret key rate of quantum repeater based on NV center decays rapidly to 300Km but in (3.4.b) when n* =50 the secret key rate of quantum repeater based on NV center decays to 400Km. This enhancement is due to high probability of emission and coupling of trapped ion quantum memory with the optical fiber.

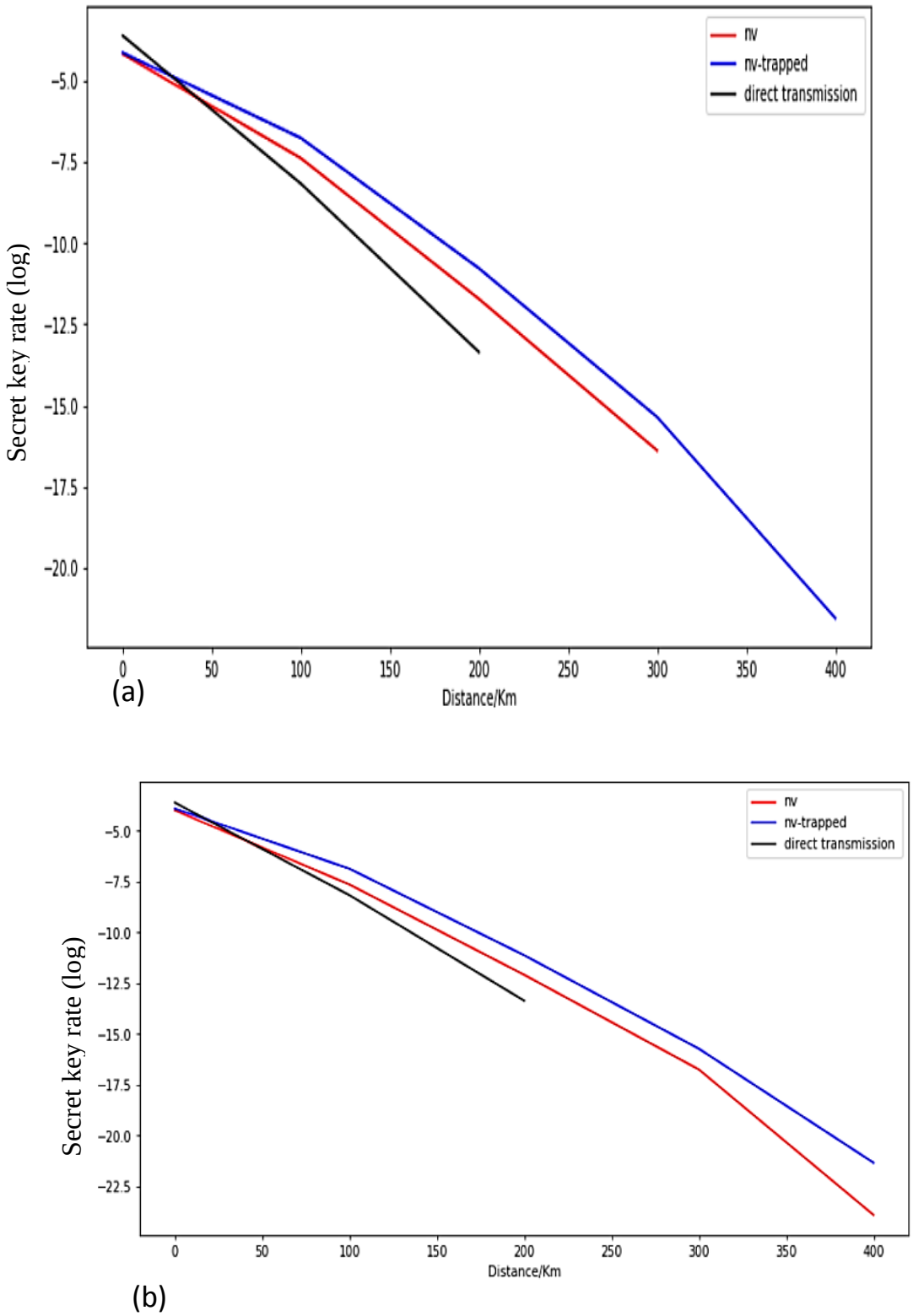

Figure 3.4: Secret key rate of quantum repeater based on NV center and NV center - trapped ion when (a) n*=100, (b) n*=50 (probability of dark count= $3*10^{-7}$).

In Figure (3.5) shows the use of trapped ion quantum memory effects on raising the probability of Bob more than the probability of Alice

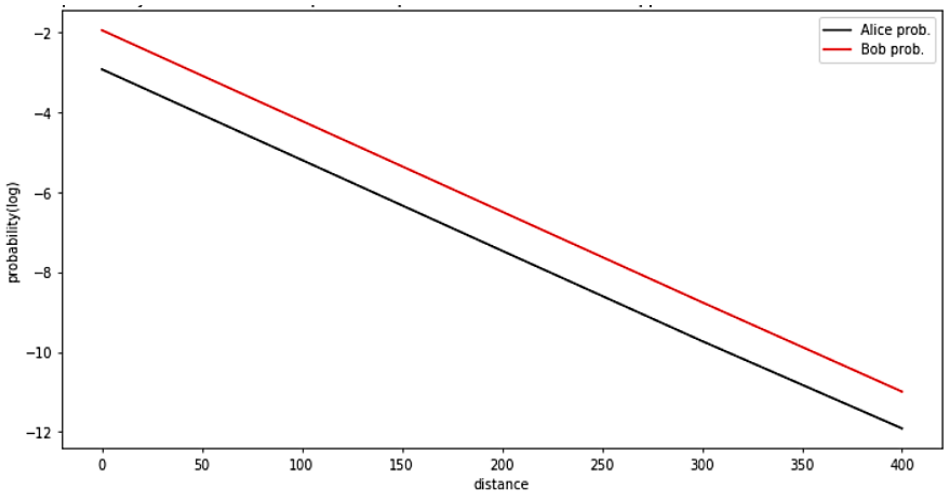

Figure 3.5: Probability of Alice and Bob in quantum repeater based on NV center - trapped ion when n*=100 (probability of dark count= $3*10^{-7}$).

Figure (3.6) shows the secret key rate that can be achieved from quantum repeater based on NV center - trapped ion. A higher key rate is obtained compared to that obtained from quantum repeater based on NV center with same number of n*, this is due to using different quantum memories when the distance that separates Alice and Bob equal to (100 Km), (200 Km) as shown in (3.6.a), (3.6.b) respectively. This means that the decrease in the n* reduce the decoherence time in the quantum memory and therefore getting a higher secret key rate.

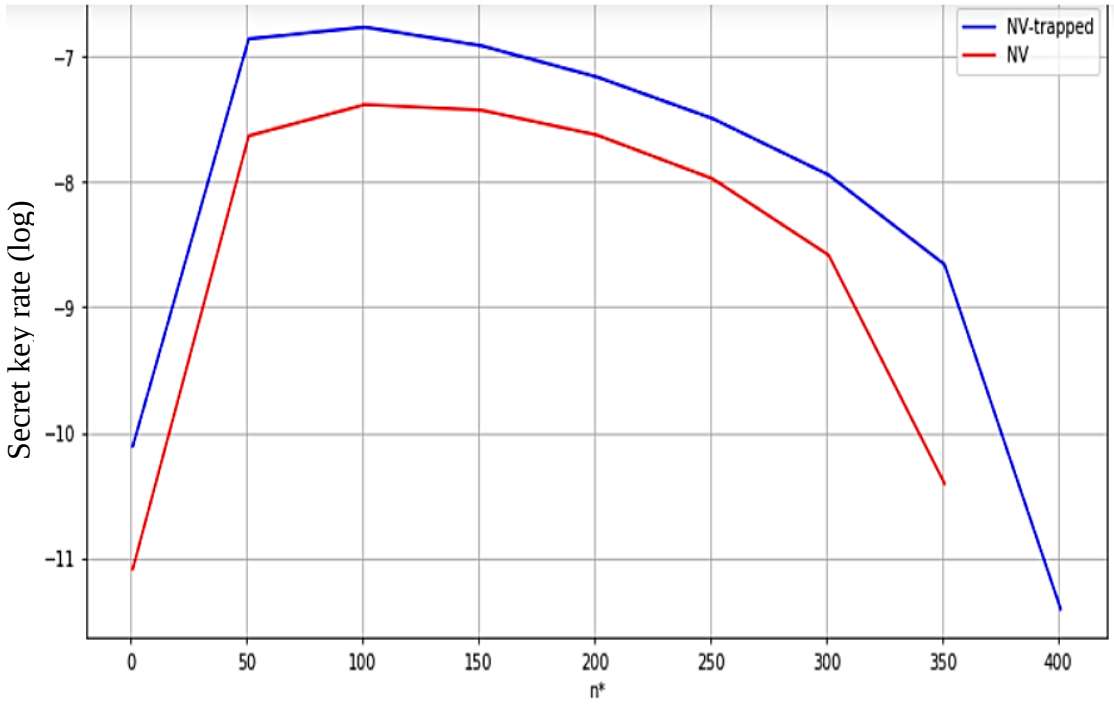

(a)

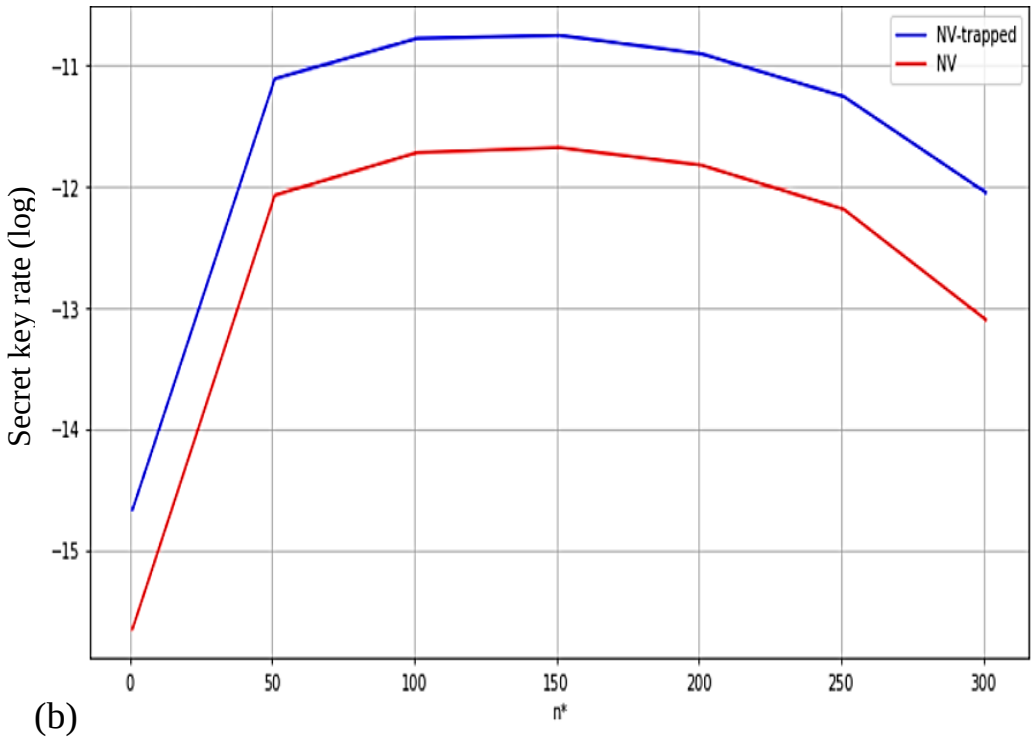

(b)

Figure 3.6: The secret key rate of quantum repeater based on NV center - trapped ion when (a) L=100Km (b) L=200Km (probability of dark count= $3*10^{-7}$).

Figure (3.7) shows the effect of quantum repeater's position that is based on NV center - trapped ion on the secret key rate. When the position of quantum repeater closer to Alice than Bob, the secret key rate with blue and red curves rapidly decreases to short distances more than the green curve which is the quantum repeater is in middle of the distance as shown in (3.7.a). In (3.7.b) the quantum repeater's position closer to Bob than Alice, also the secret key rate with blue and red curves decrease to short distance more than the other, this shows that the best position of the quantum repeater when LA=LB.

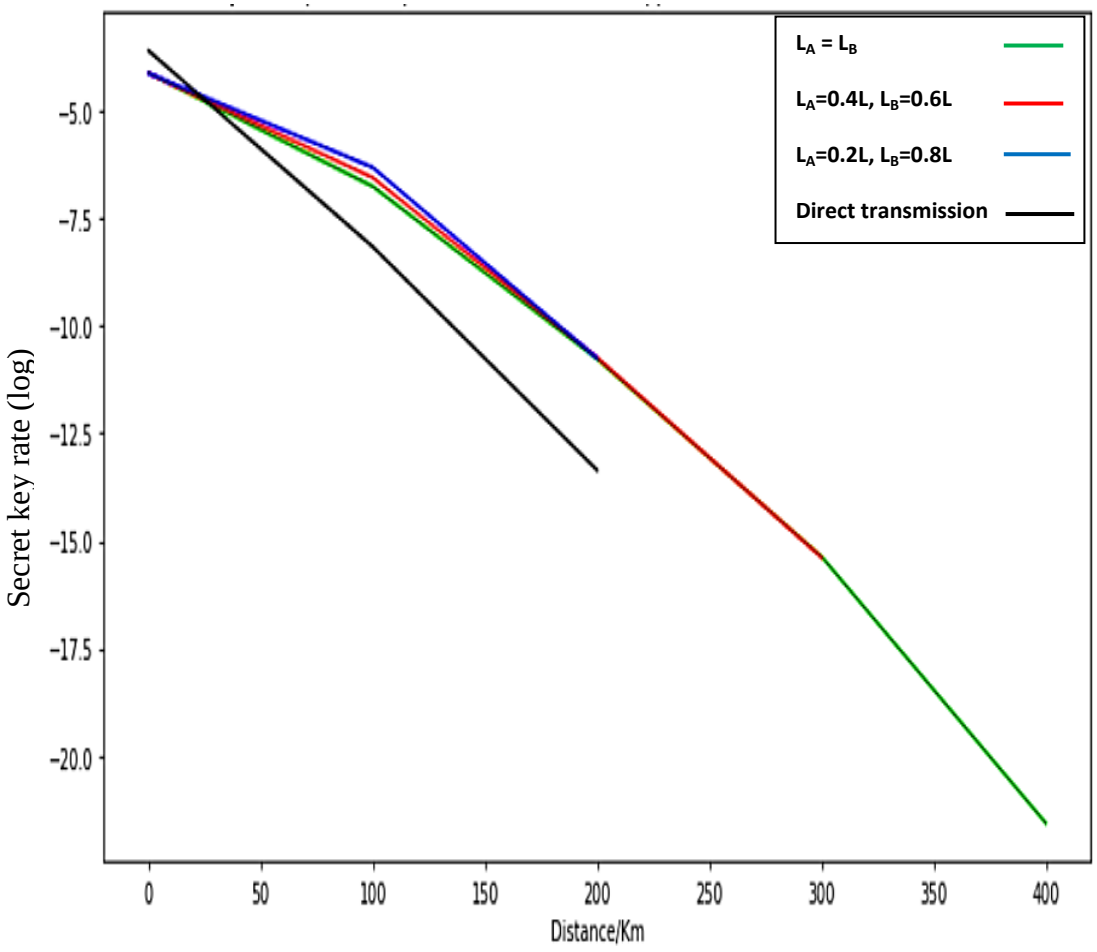

(a)

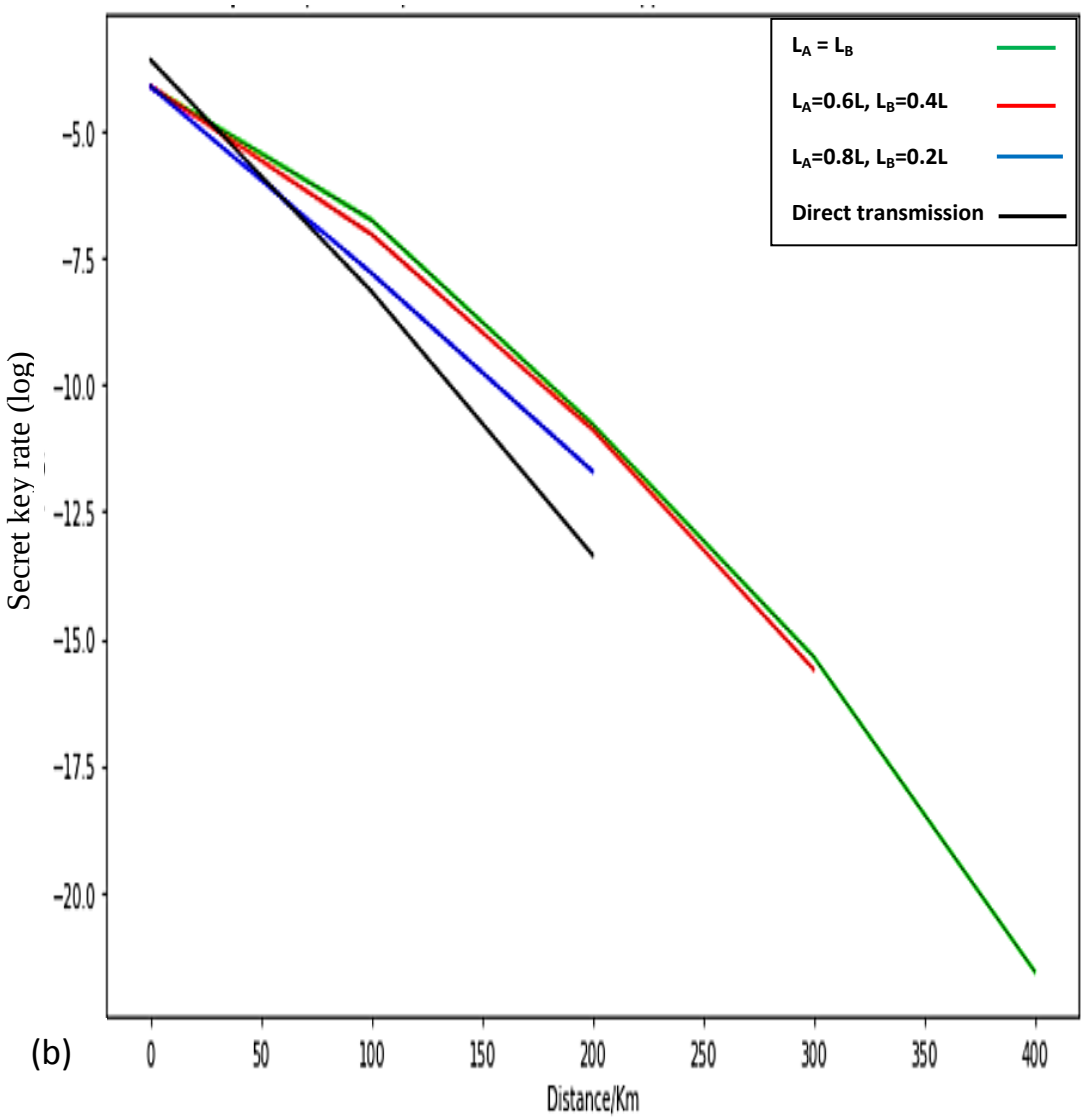

Figure 3.7: (a) the positions of quantum repeater based on NV center - trapped ion closer to Alice than Bob. (b) the positions of quantum repeater based on NV center - trapped ion closer to Bob than Alice

The dark count is another factor that effects on the secret key rate as shown in figure (3.8). At (3.8.a) the secret key rate reaches 500 Km when probability of the dark count equal to 10^{-8} , but the secret key rate decrease rapidly when probability of the dark count equal to 10^{-6} as shown in (3.8.b) because the dark count makes additional losses.

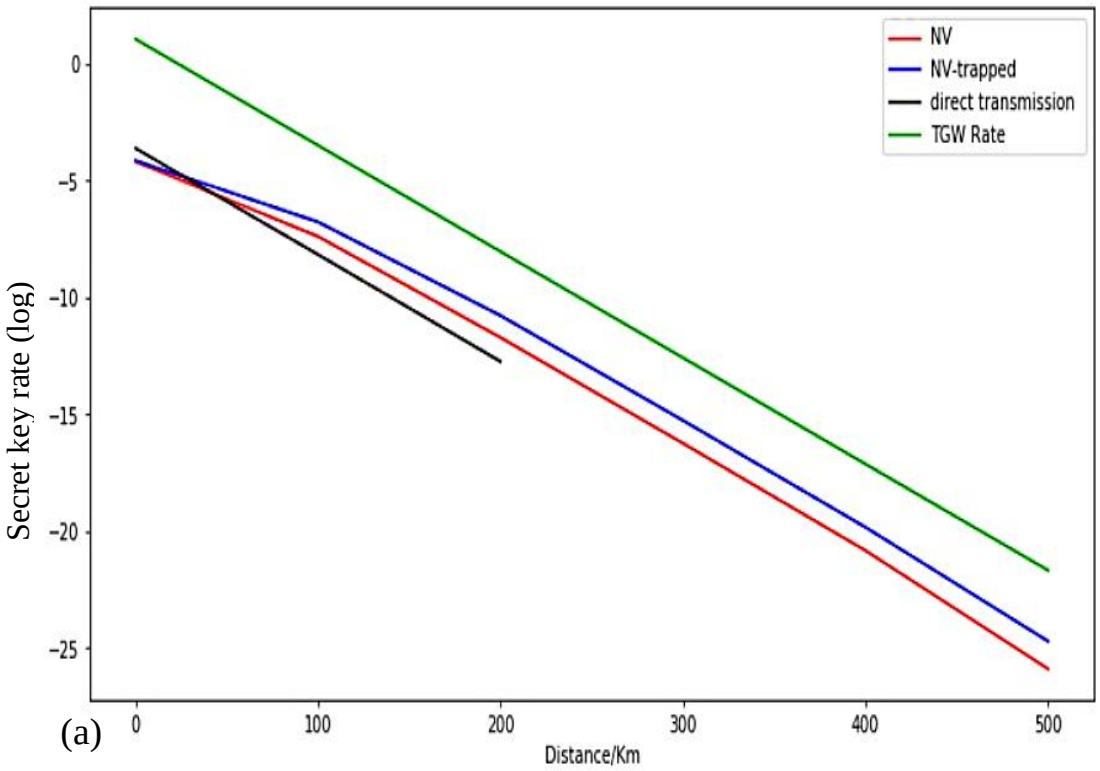

(a)

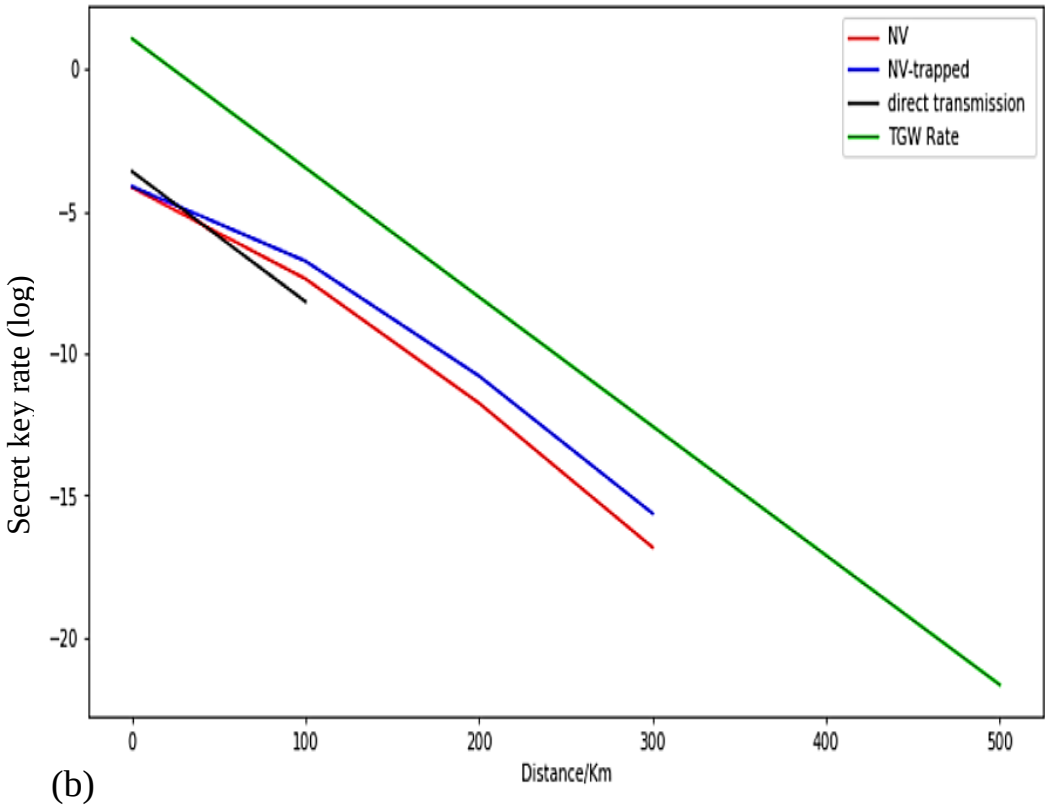

(b)

Figure 3.8: Secret key rate of quantum repeater based on NV center and NV center – trapped ion at n*=100 when (a) probability of dark count = 10^{-8} (b) probability of the dark count = 10^{-6}

3.3 Conclusion

From the results obtained from this research work, these points are concluded:

1- Using different quantum memories is better than using the position criteria of the quantum repeater to satisfy the condition (PB > PA)

2- The secret key rate of different quantum memories model is better than that of identical model and reduce the number of trails n* .

3- The scheme shows the best position of the quantum repeater is in the middle of the distance that separates Alice and Bob to maximize the secret key rate with distances**.**

3.4 Future Work

This work can be continued in the future to cover these directions of applications:

1- Using time bin coding in the cut-off protocol and study its effect on the secret key rate.

2- Using other types of the quantum memories and study their effect on the secret key rate.

3- The effect of using multi quantum repeater based on different quantum memories with cut-off, on the secret key rate.

References

[1] Bennett C. H., quantum information and computation, Phys. Today, Vol. 24 (1995).

[2] Gisin N., Thew R., Quantum Communication Technology, IET Digital Library, Vol. 46, Issue 14, p. 965 – 967, (2010)

[3] Schumacher B., Quantum Computing and Quantum Communications, Phys. Rev., A 45, 2614, (1996).

[4] van Enk S.J., Cirac J.I., Zoller P., Ideal Quantum Communication over Noisy Channels: a Quantum Optical Implementation, Phys. Rev. Lett. 78, 4293 ,(1997)

[5] Gottesman D., Lo H.-K. , Lutkenhaus N., Preskill J., Security of quantum key distribution with imperfect devices, International Symposium on Information Theory, 2004. ISIT 2004. Proceedings. , IEEE, ,(2004)

[6] Hayashi M., Practical Evaluation of Security for Quantum Key Distribution, Physical Review A, Vol. 74, 022307, (2006)

[7] Xue P., Li C.-F., Guo G-C., Efficient quantum key distribution scheme with nonmaximally entangled states, Phys. Rev., A 64, 032305, (2001)

[8] Lo H-K., Ma X., Chen K., Decoy State Quantum Key Distribution, Phys. Rev. Lett., 94, 230504, (2005)

[9] Wootters W.K. and ZurekW.H., A single quantum cannot be cloned, Nature, 299 802–3,(1982)

[10] Meter R. V., System Design for a Long-Line Quantum Repeater, IEEE Journal , Vol. 17 , 3, (2009)

[11] Briegel H-J, Dür W., Cirac J. I. and Zoller P., Quantum repeaters: the role of imperfect local operations in quantum communication, Phys. Rev. Lett. 81, 5932,(1998)

[12] William J. Munro, K. Nemoto, P.Van Loock, Y. Yamamoto, QUANTUM REPEATER , U.S. Patent , US 8,135,276 B2,(2012)

[13] Xiang G. Y. , Ralph T. C. , Lund A. P. , Walk N. & Pryde G. J., noiseless linear amplification and distillation of entanglement , Nature Photonics, vol. 4, 316–319, (2010)

[14] Vollbrecht K.H., Muschik C. A., and Cirac J. I., Entanglement Distillation by Dissipation and Continuous Quantum Repeaters Phys. Rev. Lett. 107, 120502, (2011)

[15] Watrous J., Many copies may be required for entanglement distillation , Phys. Rev. Lett, 93, 010502,(2004)

[16] Rozpędek F., Goodenough K., Ribeiro J., Kalb N., Vivoli V. C., Reiserer A., Hanson R., Wehner S., Elkouss D**,** Parameter regimes for a single sequential quantum repeater, Quantum Sci. Technol. vol 3, no 3,(2018)

[17] Imre S., Balazs F., Quantum Computing and Communications, Wiley J. & Sons Ltd, England, (2005).

[18] Nielsen M. A., and Chuang I. L., Quantum Computation and Quantum Information:10th Anniversary Edition, Cambridge University Press, New York, NY, USA, 10th edition, (2011).

[19] Imre S., Gyongyosi L., Advanced Quantum Communications, an Engineering Approach, IEEE Press Editorial Board (2012).

[20] Wootters K. W., Zurek W. H., The no-cloning theorem. American Institute of Physics, S-0031-9228-0902-350-3, (2009).

[21] Bennett C. H., Wiesner S. J., Communication via One- and Two-Particle Operators on Einstein-Podolsky-Rosen States, Phys. Rev. Lett. 69, 2881 (1992)

[22] Bennett C. H., Brassard G., et al, Teleporting an unknown quantum state via dual classical and Einstein-Podolsky-Rosen channels, Phys. Rev. Lett., 70,13, (1993)

[23] Żukowski M., Zeilinger A., Horne M. A., Ekert A. K. ,"event-ready-detectors"bell experiment via entanglement swapping. Phys. Rev. Lett., 71, 4287,(1993)

[24] Bennetta C. H., Brassard G., Quantum cryptography: Public key distribution and coin tossing, Theoretical Computer Science 560:175-179,(1984)

[25] A Survey of the Prominent Quantum Key Distribution Protocols, 2007, https://www.cse.wustl.edu/~jain/cse571-07/ftp/quantum/

[26] Gisin N., Ribordy G., Tittel W., Zbinden H., "Quantum Cryptography", Reviews of Modern Physics, vol. 74, , pp. 146 – 195, January (2002)

[27] Scarani V., et al., The security of practical quantum key distribution, Rev. Mod. Phys. 81, 1301 (2009)

[28] Lo H. K., Chau F., Ardehali M., Efficient Quantum Key Distribution Scheme and Proof of Its Unconditional Security, J. Cryptology 18, 133 (2005).

[29] Dur W., Briegel H.-J., Cirac J. I., Zoller P., Quantum repeaters based on entanglement purification, Phys. Rev. A, **59**:169–181, (1999).

[30] Deutsch D., Ekert A., Jozsa R., Macchiavello C., Popescu S., Sanpera A., Quantum privacy amplification and the security of quantum cryptography over noisy channels, Phys. Rev. Lett., **77**:2818–2821, (1996).

[31] Bennett C. H., Brassard G., Popescu S., Schumacher B., Smolin J. A., Wootters W. K., Purification of noisy entanglement and faithful teleportation via noisy channels, Phys. Rev. Lett, **76**:722–725, (1996).

[32] Sangouard N., Simon C., et al Robust and Efficient Quantum Repeater with Atomic Ensembles and Linear Optics, arXiv preprint :0802.1475v2 [quant-ph] (2008).

[33] Cirac J. I., Zoller P., Kimble H. J., and Mabuchi H., Quantum state transfer and entanglement distribution among distant nodes in a quantum network, Phys. Rev. Lett., **78**:3221, (1997).

[34] Simon C., Afzelius M., Appel J., Giroday A. B., et al, Quantum Memory, The European Physical Journal *D*, 58, 1–22,(2010)

[35] Massa N., Fiber optic telecommunication. Fundamentals of Photonics. University of Conneticut, (2000)

[36] Liu X., Akahane K., Jahan N. A., Kobayashi N.,et al, Single-photon emission in telecommunication band from an InAs quantum dot grown on InP with molecular-beam epitaxy, APPLIED PHYSICS LETTERS 103, 061114 (2013)

[37] Doherty M. W., Manson N. B., Delaney P., Jelezko F., Wrachtrup J., Hollenberg L. C., "The nitrogen-vacancy colour centre in diamond," Physics Reports, vol. 528, no. 1, pp. 1 – 45, (2013).

[38] Bar-Gill N., Pham L., Jarmola A., Budker D., Walsworth R., "Solid-state electronic spin coherence time approaching one second," Nature Communications, 4, Article number: 1743, (2013).

[39] Park Y.S., et al., Cavity QED with Diamond Nano crystals and Silica Microspheres, Nano Lett. **6**, 2075 (2006)

[40] Dutt M. V. G., Childress L., Jiang L., Togan E., Maze J., Jelezko F., Zibrov A. S., Hemmer P. R., and Lukin M. D., "Quantum Register Based on Individual Electronic and Nuclear Spin Qubits in Diamond," Science, vol. 316, no. 5829, pp. 1312–1316, (2007).

[41] Togan E., Chu Y., Trifonov A. S., et al, "Quantum entanglement between an optical photon and a solid-state spin qubit," Nature, vol. 466, pp. 730–734, (2010).

[42] Hensen B., Bernien H., Dreau A. E., Reiserer A., et al, "Loophole-free Bell inequality violation using electron spins separated by1.3 kilometres," Nature, vol. 526, pp. 682–686, 2015.

[43] Beveratos A., Brouri R., Gacoin T., et al, Single Photon Quantum Cryptography, Phys. Rev. Lett., vol. 89, p. 187901, Oct 2002.

[44] Paul W., Electromagnetic traps for charged and neutral particles, Rev. Mod. Phys. 62, 531, (1990)

[45] "Introduction to Ion Trap Quantum Computing ,University of Oxford Department of Physics, www2.physics.ox.ac.uk.Retrieved 2018-11-05

[46] Schindler P., Nigg D., Monz T., et al, A quantum information processor with trapped ions, New J. Phys. 15 123012, (2013)

[47] Kim Y.-H., Kulik S.P., Shih Y., Quantum Teleportation with a Complete Bell State Measurement, Phys. Rev. Lett. 86, 1370, (2001)

[48] Christ A., Brecht B., Mauerer W., Silberhorn C., Theory of quantum frequency conversion and type-II parametric down-conversion in the high-gain regime, New Journal of Physics 15 053038 (27pp) ,(2013)

[49] Luong D., Jiang L., Kim J., and Lutkenhaus N., Overcoming lossy channel bounds using a single quantum repeater node, Appl. Phys., B, 122 (4):96, (2016).

[50] Mastromattei C., Assessing the Practicality of a Simple Multi-node Quantum Repeater, MSc Thesis, University of Waterloo, Ontario, Canada, (2017).

[51] kadhim A. N., Hasan J.A, Analysis of a Quantum Repeater Scheme Based on Non-Identical Quantum Memories, (2018)

[52] Balance C. J., Schafer V. M., Home J. P., Szwer D. J., et al, Hybrid quantum logic and a test of Bell's inequality using two different atomic isotopes, Nature **528**, 384–386 ,17 (2015)

[53] Tan T. R., Gaebler J. P., Lin Y., Wan Y., Bowler R., Leibfried D., and Wineland D. J., Multi-element logic gates for trapped-Ion qubits, Nature **528**, 380–383 ,17 (2015)

[54] Kurtsiefer C., Mayer S., Zarda P., Weinfurter H., Stable Solid-State Source of Single Photons, Physical Review Letters, vol 85, 290, (2000)

[55] Harty T. P., Allcock D. T. C., Ballance C. J., Guidoni L., Janacek H. A., Linke N. M., Stacey D. N., Lucas D. M, High-Fidelity

Preparation, Gates, Memory, and Readout of a Trapped-Ion Quantum Bit , Physical Review,(2014)

[56] Tamura Y., Sakuma H., Morita K., Suzuki M., Yamamoto Y., Shimada K., Honma Y, Sohma K., Fujii T. and Hasegawa T., The First 0.14-dB/km Loss Optical Fiber and its Impact on Submarine Transmission , Journal of Lightwave Technology, Vol. 36, Issue 1, pp. 44-49 (2018)

[57] Bock M., Eich P., Kucera S., Kreis M., Lenhard A., Becher C., Eschner J., High-fidelity entanglement between a trapped ion and a telecom photon via quantum frequency conversion Nature Communications volume 9, Article number: 1998, (2018)

[58] Riedel D., Söllner I., Shields B. J., Starosielec S., Appel P., Neu E., Maletinsky P., Warburton R. J., Deterministic Enhancement of Coherent Photon Generation from a Nitrogen-Vacancy Center in Ultrapure Diamond, Physical Review X 7, 031040,(2017)

[59] Brandstätter B., McClung A., Schüppert K., Casabone B.and and et al, Integrated fiber-mirror ion trap for strong ion-cavity coupling, Review of scientific instruments, 84, 123104, (2013)

[60] Paschotta R. Article on ‘fibers’ in Encyclopedia of Laser Physics and Technology Available online:https://rp- photonics.com/fibers.html

[61] Pfister A. D., Salz M. and et al,A quantum repeater node with trapped ions: a realistic case example, Appl. Phys. B, 122:89, (2016)

[62] Reiserer A., Kalb N., Blok M. S., Bemmelen K. J. M., Taminiau T. H., Hanson R., Robust Quantum-Network Memory Using Decoherence-Protected Subspaces of Nuclear Spins, Physical Review X 6, 021040, (2016)

[63] Maurer P. C., Kucsko G., Latta C., Jiang L., Yao N. Y., Bennett S. D. and et al, Room Temperature Quantum Bit Memory Exceeding One Second , Science ,Vol. 336, Issue 6086, pp. 1283-1286, (2012)

[64] Zaske S. et al , Visible-to-telecom quantum frequency conversion of light from a single quantum emitter, Phys. Rev. Lett.,109, 147404, (2012)

[65] Walker T., Miyanishi K., Ikuta R. and et al, Long-distance single photon transmission from a trapped ion via quantum frequency conversion, Phys. Rev. Lett., 120, 203601, (2018)

[66] Darqui´e. B, Jones M. PA , Dingjan J., Beugnon J., Bergamini S., Sortais Y., Messin G., Browaeys A., Grangier P., Controlled Single-Photon Emission from a Single Trapped Two-Level Atom, *Science*, 309, 5733, 454-456, (2005)

[67] Pfaff W., et al, Unconditional quantum teleportation between distant solid-state quantum bits, Science, 345, 6196, 532-535, (2014)

[68] Takeoka M., Guha S., Wilde M. M., The squashed entanglement of a quantum channel, IEEE, 60, 4987. (2014)

الخلاصة

ان الهدف من أي نظام اتص ال هو نقل المعلومات عبر مسافات طويلة مع اقل خطأ. لسوء الحظ ، فإن نقل المعلومات مباشرة بين نقطتين (اليس وبوب) المتصلين بالألياف الضوئية مستحيل بسبب الاضمحلال الأسي لكفاءة انتقال الضوء مع طول الألياف الضوئية. وبالتالي ، للتغلب على هذه المشكلة ، يجب تقسيم هذه المسافة إلى مسافات صغيرة عن طريق إدخال محطة وسيطة بينهما ؛ وتعرف هذه المحطة باسم مكرر الكم

واحدة من مخططات المكرر الكمي تستخدم مفهوم القطع بذاكرات كمية متطابقة في مكرر الكم ، أي أن المكرر الكمي يرسل فوتونًا متشابكًا واحدًا مع الذاكرة الكمومية الأولى إلى (أليس) لمرات عديدة حتى يتم الكشف عن الفوتون ، ثم يرسل المكررالكم فوتونا متشابكا مع الذاكرة الكمية الثانية إلى بوب لعدد محدد من الممرات (قطع) إذا قام بوب بالكشف قبل القطع ، يتم تطبيق قياس حالة بيل وإذا لم يحدث ذلك ، سيتم إحباط الجولة والبدء من جديد. يقلل هذا البروتوكول من عدم ترابط ذاكرات الكم مع مرور الوقت ، من أجل تنفيذ هذا البروتوكول ، يجب أن يكون احتمال بوب للكشف عن الفوتون أكبر من أو يساوي احتمال أليس. في الفكرة الأصلية ، تكون احتمالات أليس وبوب متساوية بسبب استخدام نفس النوع من الذاكرة الكمية وتبقى هذه المساواة في حال تم استخدام أي نوع من الذاكرة الكمية.لذلك من اجل جعل احتمال بوب للكشف عن الفوتون أكبر من احتمال أليس ، يُقترح استخدام ذاكرنتي كمية مختلفة في مكرر الكم للحصول على أفضل عدد من القطع وتعظيم معدل المفتاح السري. تم الحصول على معدل المفتاح السري $1.04372442*10^{-3}$ ، $1.47772778*10^{-5}$ لرقم القطع 50 و$1.15652165*10^{-3}$ ، $2.08223733*10^{-5}$ لرقم القطع 100 للمسافة 100 كم و 200 كم على التوالي.

وزارة التعليم العالي والبحث العلمـي
جامعـــــــــــة بغـــــــــداد
معهـــــد الليـــزر للدراسات العليـا

تحسين أداء مكرر الكم باستخدام ذاكرتين غير متطابقة المعتمدةعلى مفهوم القطع

رسالة مقدمة الى
معهد الليزر للدرات العليا /جامعة بغداد/ لأستكمال نيل شهادة الماجستير علوم في الليزر/ الهندسة الألكترونية والاتصالات

من قبل
مـــروة أسعـــد خالـــد
بكلوريوس الهندسة الالكترونية والاتصالات
2009

بأشراف
م.د جـواد عبـد الكاظـم حسـن

1441هـ 2019م